

Spatial patterns in glacier characteristics and area changes from 1962 to 2006 in the Kanchenjunga-Sikkim area, eastern Himalaya

Adina E. Racoviteanu^{1,*}, Y. Arnaud^{1,2}, Mark W. Williams³ and William F. Manley⁴

¹*Laboratoire de Glaciologie et Géophysique de l'Environnement, 54, rue Molière, Domaine Universitaire, BP 96 38402 Saint Martin d'Hères cedex, France*

²*Laboratoire d'Étude des Transferts en Hydrologie et Environnement, BP 53 38401 Saint Martin d'Hères cedex, France*

³*Department of Geography and Institute of Arctic and Alpine Research, University of Colorado, Boulder CO 80309*

⁴*Institute of Arctic and Alpine Research, University of Colorado, Boulder CO 80309*

Abstract

This study investigates spatial patterns in glacier characteristics and area changes at decadal scales in the eastern Himalaya: Nepal (Arun and Tamor basins), India (Tista basin in Sikkim), and parts of China and Bhutan based on various satellite imagery: Corona KH4 imagery, Landsat 7 Enhanced Thematic Mapper Plus (ETM+) and Advanced Spaceborne Thermal Emission Radiometer (ASTER), QuickBird (QB) and WorldView-2 (WV2). We compare and contrast glacier surface area changes 1962 – 2000/2006 and their dependency on glacier topography (elevation, slope, aspect, percent debris cover), climate (solar radiation and precipitation) on the eastern side (Sikkim) versus the western side (Nepal).

Glacier mapping from 2000 Landsat ASTER yielded $1,463 \pm 88 \text{ km}^2$ total glacierized area, of which $569 \pm 34 \text{ km}^2$ was located in Sikkim and $488 \pm 29 \text{ km}^2$ in eastern Nepal. Supraglacial debris covered 11% of the total glacierized area, and supraglacial lakes covered about 5.8% of the debris-covered glacier area. Glacier area change (1962 to 2000) was $-0.50 \pm 0.2\% \text{ yr}^{-1}$, with little difference between Nepal ($0.53 \pm 0.2\% \text{ yr}^{-1}$) and Sikkim ($0.44 \pm 0.2\% \text{ yr}^{-1}$). Glacier area change was controlled mostly by glacier area, elevation, altitudinal range and to a smaller extent slope and aspect. In the Kanchenjunga-Sikkim area, we estimated a glacier area change of $-0.23 \pm 0.08\% \text{ yr}^{-1}$ from 1962 to 2006 based on high-resolution imagery. On a glacier-by-glacier basis, clean glaciers exhibit more area loss on average from

1 1962 to 2006 (34%) compared to debris-covered glaciers (22%). Glaciers in this region of the
2 Himalaya area are shrinking at similar rates to those reported for the last decades in other
3 parts of the Himalaya, but individual glacier rates of change vary across the study area with
4 respect to local topography, percent debris cover or glacier elevations.

5

6 **1. Introduction**

7

8 Himalayan glaciers have generated a lot of concern in the last few years, particularly with
9 respect to potential consequences of glacier changes on the regional water cycle (Immerzeel
10 et al. 2010; Kaser et al. 2010; Immerzeel et al. 2012; Racoviteanu et al. 2013a). In the last
11 decades, the availability of low-cost data from optical remote sensing platforms with global
12 coverage provided opportunities for glacier mapping at regional scales. Remote sensing
13 techniques have helped improve estimates of glacier area changes (Bajracharya et al. 2007;
14 Bolch 2007; Bolch et al. 2008a; Bhambri et al. 2010; Kamp et al. 2011), glacier lake changes
15 (Wessels et al. 2002; Bajracharya et al. 2007; Bolch et al. 2008b; Gardelle et al. 2011) and
16 region-wide glacier mass balance (Berthier et al. 2007; Bolch et al. 2011; Kääb et al. 2012;
17 Gardelle et al. 2013), but significant gaps do remain. The new global Randolph Glacier
18 Inventory (RGI) v.4 (Pfeffer et al. 2014) provides a global dataset of glacier outlines intended
19 for large-scale studies; however, in some regions the quality varies, and the outlines may not
20 be suitable for detailed regional analysis of glacier parameters. A new Landsat-based
21 inventory has been compiled using imagery from 1999 to 2003, which along with the current
22 study, may help improve the accuracy in some areas of RGI (Nuimura et al. 2014). Some
23 other regional glacier inventories have been constructed in the past, for example for the
24 western part of the Himalaya (e.g. Bhambri et al. 2011; Kamp et al. 2011; Frey et al. 2012),
25 but only a few are available for the eastern extremity of the Himalaya (e.g. Bahuguna 2001;

1 Krishna 2005; Bajracharya and Shrestha 2011; Basnett et al. 2013). The use of remote
2 sensing for glacier mapping in this area is limited by frequent cloud cover and sensor
3 saturation due to unsuitable gain settings and the persistence of seasonal snow, which
4 hampers quality satellite image acquisition. Furthermore, this area has very limited reliable
5 baseline topographic data needed for glacier change detection, as discussed in detail in
6 Bhambri and Bolch (2009a). The earliest Indian glacier maps date from topographic surveys
7 conducted by expeditions in the mid-nineteenth century (Mason 1954), but these are limited
8 to a few glaciers. The Geologic Survey of India (GSI) inventory based on 1970s Survey of
9 India maps (Shanker 2001; Sangewar and Shukla 2009) is not in the public domain. For
10 eastern Nepal, 1970's topographic maps from Survey of India 1:63,000 scale are available,
11 but their accuracy is not known with certainty. Given these limitations, declassified Corona
12 imagery from the 1960s and 1970's has increasingly been used to develop baseline glacier
13 datasets, for example in the Tien Shan (Narama et al. 2007), Nepal Himalaya (Bolch et al.
14 2008a) and parts of Sikkim Himalaya (Raj et al. 2013).

15 The topographic and climatic controls on glacier surface area have received increasing
16 attention in recent studies, particularly with respect to debris-covered glaciers (Bolch et al.
17 2008a; Salerno et al. 2008; Basnett et al. 2013; Thakuri et al. 2014). Some studies have
18 characterized the small-scale glacier surface topography of debris-covered glaciers using
19 field-based surveys (Iwata et al. 2000; Sakai and Fujita 2010; Zhang et al. 2011), while other
20 studies focused on understanding patterns at the mountain-range scale (Scherler et al. 2011;
21 Bolch et al. 2012; Gardelle et al. 2013; Racoviteanu et al. 2014). Glacier shrinkage and mass
22 loss has been documented in the Himalaya concomitantly with an increase in debris cover
23 (Bolch et al. 2011; Nuimura et al. 2012). However, the influence of debris cover on glacier
24 mass balance remains debatable (Scherler et al. 2011; Kääb et al. 2012), and modeling of
25 melt under the debris cover is subject to uncertainties due to limited field-based

1 measurements of debris thickness needed for model parameterization (Mihalcea et al. 2008a;
2 Mihalcea et al. 2008b; Zhang et al. 2011; Foster et al. 2012).

3 While significant progress has been made in the recent years on remote sensing glacier
4 mapping in the Himalaya, some of the sub-regions still need updated glacier area and surface
5 characteristics including debris cover. The objective of this study is two-fold: (1) present the
6 current glacier distribution and characteristics in a data-scare area of the eastern Himalaya
7 based on an updated 2000 Landsat ETM+ and ASTER inventory, along with elevation data
8 from the Shuttle Radar Topography Mission (SRTM); (2) investigate spatial patterns in
9 glacier surface area changes from 1962 (Corona KH4) to 2000 (Landsat/ASTER) and 2006
10 (QB) 2006 (WV2) and their dependence on topographic and climatic factors, with a
11 particular emphasis on debris-covered glacier tongues. These updated glacier datasets help
12 fill a gap in global glacier inventories such as the RGI (Pfeffer et al. 2014), as well as for
13 subsequent future mass balance applications at regional scales.

14 **2. Study area**

15 The study area encompasses glaciers in the eastern Himalaya ($27^{\circ} 04' 52''$ N to $28^{\circ} 08'$
16 $26''$ N latitude and $88^{\circ} 00' 57''$ E to $88^{\circ} 55' 50''$ E longitude), located on either side of the
17 border between Nepal and India in the Kanchenjunga-Sikkim area (Fig. 1). Based on SRTM
18 data, relief in this area ranges from 300 m at the bottom of the valleys to 8,598 m (Mt.
19 Kanchenjunga). Valley glaciers cover about 68% of the glacierized area, mountain glaciers
20 cover 28%, and the remaining are cirque glaciers and aprons (Mool et al. 2002). The glacier
21 ablation area is typically covered by heavy debris-cover originating from rockfall on the steep
22 slopes (Mool et al. 2002), reaching up to a thickness of several meters at the glacier termini
23 (Kayastha et al. 2000). The eastern part of this area constitutes the Sikkim province of India,
24 and the western part is located in eastern Nepal, and encompasses the Tamor and parts of
25 Arun basin. Climatically, this area of the Himalaya is dominated by the South Asian summer

1 monsoon circulation system (Bhatt and Nakamura 2005) caused by the inflow of moist air
2 from the Bay of Bengal to the Indian subcontinent during the summer (Yanai et al. 1992;
3 Benn and Owen 1998). The Himalaya and Tibetan plateau (HTP) acts as a barrier to the
4 monsoon winds, bringing about 77% of precipitation on the south slopes of the Himalaya
5 during the summer months (May to September) (Fig. 2). This climatic particularity causes a
6 “summer-accumulation” glacier regime type, with accumulation and ablation occurring
7 simultaneously in the summer (Ageta and Higuchi 1984). In Sikkim, rainfall amounts range
8 from 500 to 5000 mm per year, with annual averages of 3,580 mm recorded at Gangtok
9 station (1,812 m) (1951 to 1980) (IMD 1980), and 164 rainy days per year (Nandy et al.
10 2006). Mean minimum and maximum daily temperatures at Gangtok station were reported as
11 11.3°C and 19.8°C, with an average of 15.5°C based on the same observation record (IMD
12 1980).

13 *[Fig. 1 – 2]*
14

15 **3. Methodology**

16 *3.1. Data sources*

17 Satellite imagery 18

19 Remote sensing datasets used in this study are summarized in Table 1, and included: 1)
20 baseline remote sensing data from Corona declassified imagery (year 1962); 2) “reference”
21 datasets for 2000s from Landsat ETM+ and ASTER and 3) high-resolution imagery from QB
22 (2006) and WV (2009), all described below.

23 (1) Corona KH4 scenes (1962) were obtained from the US Geological Survey EROS Data
24 Center (USGS-EROS 1996). The Corona KH4 system was equipped with two panoramic
25 cameras (forward-looking and rear-looking with 30 degrees separation angle), and acquired
26 imagery from February 1962 to December 1963 (Dashora et al. 2007). We chose images

1 from the end of the ablation season (October/November in this part of the Himalaya), suitable
2 for glaciologic purposes. Six Corona stripes were scanned at 7 microns by USGS from the
3 original film strips, with a reported nominal ground resolution of 7.62 m (Dashora et al.
4 2007). Corona images are known to contain significant geometric distortions due to cross-
5 path panoramic scanning. The Frame Ephemeris Camera and Orbital Data (FECOD)
6 camera/spacecraft parameters (roll, pitch, yaw, speed, altitude, azimuth, sun angle and film
7 scanning rate) for Corona missions, needed to construct a camera model and to correct these
8 distortions, are not easily available. To orthorectify the scenes, we defined a non-metric
9 camera model in ERDAS Leica Photogrammetric Suite (LPS), with focal length, air photo
10 scale and flight altitude extracted from the declassified documentation of the KH4 mission
11 (Dashora et al. 2007). We used the bundle block adjustment procedure in LPS to
12 simultaneously estimate the orientation of all the CORONA stripes on the basis of 117
13 ground control points (GCPs) extracted from the panchromatic band of the 2000 Landsat
14 ETM+ image (15 m spatial resolution). GCPs (x,y) were identified on the Landsat image on
15 non-glacierized terrain including moraines, river crossings, and outwash areas, and elevation
16 information (z) were extracted from the SRTM DEM v.4 (CGIAR-CSI 2004). Tie points
17 (TPs) were automatically extracted in LPS and visually checked from overlapping Corona
18 strips, on the Landsat image. The Corona stripes were mosaicked in ERDAS LPS to produce
19 the final orthorectified image, with a horizontal accuracy (RMSE_{x,y}) of the bundle block
20 adjustment of 10.5 m. The orthorectification process of the 1962 Corona yielded a RMSE_{x,y}
21 error of ± 10 m, and the actual “ground” RMSE_{x,y} of the Corona block of ~ 60 m. A trend
22 analysis on the horizontal shifts between Corona and the reference Landsat scene showed that
23 the largest errors occurred towards the edges of the images, mostly outside the glaciers, and
24 did not impact the area change analysis.

1 (2) The orthorectified Landsat ETM+ scene from December 2000, obtained from the
2 USGS Eros Data Center was the main dataset for the updated glacier inventory. In addition,
3 six orthorectified ASTER products (2000 to 2002) were obtained at no cost through the
4 Global Land Ice Monitoring from Space (GLIMS) project (Raup et al. 2007). Images were
5 selected at the end of the ablation season for minimal snow, and had little or no clouds. Five
6 of these scenes were used for on-screen manual corrections of the Landsat-based glacier
7 outlines in challenging areas where shadows or clouds obstructed the view of the glaciers. In
8 addition, the surface kinetic temperature product (AST08) product from the November 27th,
9 2001 ASTER scene was used for clean ice delineation of debris cover along with topographic
10 information using a decision-tree algorithm (Racoviteanu and Williams 2012). The October
11 29th, 2002 scene, covering the Kanchenjunga-Sikkim area east and west of the topographic
12 divide, was used to investigate the spatial distribution of surface temperature over selected
13 debris covered tongues.

14 (3) Two QB scenes from January 2006 were obtained from Digital Globe as ortho-ready
15 standard imagery (radiometrically calibrated and corrected for sensor and platform
16 distortions) (Digital_Globe 2007). These scenes, covering an area of 1,107 km² were well-
17 contrasted and mostly snow-free outside the glaciers. We orthorectified these scenes in
18 ERDAS Imagine Leica Photogrammetry Suite (LPS) using Rational Polynomial Coefficients
19 (RPCs) provided by Digital Globe and the SRTM DEM, and mosaicked them in ERDAS
20 Imagine. The scenes were resampled to 3 m-pixel size during the orthorectification process
21 using the cubic convolution method suitable for continuous raster data, in order to reduce
22 disk space and processing time. One WorldView-2 (WV2) panchromatic, ortho-ready scene
23 at 50 cm spatial resolution from Dec 02, 2010 was also obtained to cover the terminus of
24 Zemu glacier, which was missing from the QB extent. All datasets were registered to UTM
25 projection zone 45N, with elevations referenced to the WGS84 datum.

1 *[Table 1]*

2 Elevation datasets

3 Two elevation datasets were used in this study:

4 (1) The hydrologically-sound, void-filled CGIAR SRTM DEM (90 m spatial resolution)
5 (CGIAR-CSI 2004) was used to extract glacier parameters for 2000. The SRTM dataset is
6 known to have biases on steep slopes and at higher elevations (Berthier et al. 2006; Fujita et
7 al. 2008; Nuth and Kääb 2011), as well as due to radar penetration on snow (Gardelle et al.
8 2012b). For this area, the vertical accuracy of the SRTM DEM, calculated as root mean
9 square (RMSEz) with respect to 25 field-based GCPs, was 31 m ± 10 m. The GCPs were
10 obtained in the field on non-glacierized terrain including roads and bare land outside the
11 glaciers using a Trimble Geoexplorer XE series.

12 (2) The Swiss topographic map (1:150,000 scale), compiled from Survey of India maps
13 from the 1960s, published by the Swiss Foundation for Alpine Research was used for manual
14 corrections of the 1962 Corona glacier outlines to discard any seasonal snow, to correct
15 shadow areas or bright water bodies that could be mis-classified as ice. The exact month or
16 year of each quadrant, or of the original air photos is not known with certainty because the
17 original large-scale Indian topographic maps at this scale are restricted within 100 km of the
18 Indian border, and are therefore inaccessible (Srikantia 2000; Survey_of_India 2005),
19 however this map was useful for manual corrections of the Corona outlines.

20 *3.2 Analysis extents*
21

22 We defined three analysis extents for our study area (Fig. 1 and Table 2):

23 (1) The Landsat/ASTER domain includes the Sikkim province of India, parts of
24 eastern Nepal (Tamor and Arun basins), as well as parts of Bhutan and China (Table 2). This
25 domain was used to construct the updated 2000 glacier inventory.

1 **[Table 2]**

2 The Landsat/ASTER domain was split into four sub-regions on the basis of east-west
3 and north-south climate/topographic/political barriers, as shown in Fig. 3. Rainfall averages
4 from the Tropical Rainfall Measuring Mission (TRMM) data 2B31 product (Bhatt and
5 Nakamura 2005; Bookhagen and Burbank 2006) were used to characterize the sub-regions
6 climatically. The dataset contains rainfall estimates calibrated with ground-control stations
7 derived from local and global gauge stations (Bookhagen and Burbank 2006) with a spatial
8 resolution of 0.4 degree, or ~5 km. Given the well-known biases in the TRMM data
9 (Bookhagen and Burbank 2006; Andermann et al. 2011; Palazzi et al. 2013), here we are not
10 concerned with the absolute values of gridded precipitation, but only with characterizing the
11 sub-regions in our study area using relative rainfall values. TRMM data integrated over 10
12 years (1998 to 2007) show differences in precipitation patterns among the four regions, and
13 justifies our choice of spatial domains (Table 3). The eastern side of the study area (Sikkim)
14 receives higher precipitation amounts than the western side (Nepal) (977 mm/yr versus 805
15 mm/yr). There is a pronounced north-south gradient in precipitation, with the lowest amount
16 of precipitation noticeable on the China side (146 mm/yr) (Table 3).

17 **[Fig. 3 and Table 3]**

18 (2) The Corona spatial domain is a subset of the Landsat/ASTER domain, which was
19 covered by the 1962 Corona image. Glacier surface area changes and their dependence on
20 climate and topography were computed for this extent between two time steps: the 1960s
21 decade (represented by Corona imagery), and 2000s decade (represented by
22 Landsat/ASTER). Glaciers from Bhutan in the east and China in the north were not covered
23 by the Corona image, so the area change analysis only focused on glaciers of Sikkim and
24 eastern Nepal, east and west of the topographic divide.

1 (3) The Kanchenjunga/Sikkim domain is a smaller subset covered by all three datasets
2 (Landsat/ASTER, Corona and Quickbird), allowing us to extend the glacier change analysis
3 to 2006. It comprises of 50 glaciers from the Tamor basin (Nepal) and Zemu basin (Sikkim,
4 India), located on the southern slopes of the Himalaya. The high-resolution 1962 and 2006
5 imagery was used here for to illustrate glacier area changes at a smaller scale, to show surface
6 characteristics of debris-covered glaciers, and as means to evaluate mapping of debris-
7 covered glaciers.

8 *3.3 Glacier delineation and analysis*

9
10 For the 1960s, clean glacier outlines were extracted from the panchromatic Corona
11 imagery by thresholding the digital numbers ($DN > 200 = \text{snow/ice}$), chosen based on visual
12 interpretation. Debris-covered glacier tongues were delineated manually on the basis of
13 lateral moraines and other visual clues such as supra-glacial lakes. A 5x5 median filter was
14 used to remove noise (isolated pixels from snowfields or internal rocks), as recommended in
15 other studies (Andreassen et al. 2008; Racoviteanu et al. 2009). Ice polygons with area < 0.02
16 km^2 were not considered valid glaciers and were excluded from the analysis. Manual
17 corrections were applied subsequently on the basis of the topographic map using on-screen
18 digitizing in areas of poor contrast or transient snow/clouds, which obstructed the view of
19 glaciers.

20 For the 2000s, glaciers were delineated from the Landsat ETM+ scene using the
21 Normalized Difference Snow Index (NDSI) (Hall et al. 1995), with a threshold of 0.7 (NDSI
22 $> 0.7 = \text{snow/ice}$). The NDSI algorithm relies on the high reflectivity of snow and ice in the
23 visible to near infrared (VNIR) wavelengths (0.4 – 1.2 μm), compared to their low
24 reflectivity in the shortwave infrared (SWIR, 1.4 - 2.5 μm) (Dozier 1989; Rees 2003).
25 Compared to other band ratios (Landsat $\frac{3}{4}$ and $\frac{3}{5}$), the NDSI glacier map was cleaner and
26 less noisy and was therefore preferred (Racoviteanu et al. 2008b). A 5x5 median filter was

1 used here as well to remove remaining noise, and a few areas were adjusted manually on the
2 basis of the ASTER images, notably frozen lakes misclassified as snow/ice, and some
3 glaciers underneath low clouds in the southern part of the image. Some transient snow
4 persisting in the deep shadowed valleys was manually removed from the glacier outlines on
5 the basis of the topographic map. Debris-covered glacier tongues were delineated using
6 multispectral data (band ratios, surface kinetic temperature and texture) from the Nov 27,
7 2001 ASTER scene combined with topographic variables in a decision tree, as described in
8 Racoviteanu and Williams (2012).

9 For the QB (2006) image, clean ice surfaces were delineated using band ratios $\frac{3}{4}$, then
10 isodata clustering with a threshold of 1.07 (snow/ice > 1.07), and a majority filter of 7x7 to
11 remove noise. Debris-covered tongues for this dataset were delineated manually on the basis
12 of supraglacial features (lakes and ice walls), along with lateral and frontal moraines visible
13 on the high resolution images. We also mapped supraglacial lakes from this high-resolution
14 data based on band ratios, along with texture analysis.

15 For all inventories in the Landsat/ASTER domain, ice masses were separated into glaciers
16 on the basis of the SRTM DEM, using hydrologic functions in an algorithm developed by
17 Manley (2008), described in Racoviteanu et al. (2009). Glacier area, terminus elevation,
18 maximum and median elevation, average slope angle and aspect were extracted on a glacier-
19 by-glacier basis using zonal functions on the SRTM DEM. Average glacier thickness and
20 were calculated from mass turnover principles and ice flow mechanics by Huss and Farinotti
21 (2012), based on the approach of Farinotti (2009). Their method used our glacier outlines and
22 the SRTM DEM to derive thickness and length estimates iteratively based on Glenn's flow
23 law and a shape factor (Paterson 1994). For simplicity and consistency for change analysis,
24 we assumed no shift in the ice divides over the period of analysis, and excluded all nunataks
25 and snow-free steep rock walls from the glacier area calculations. Bodies of ice above the

1 bergschrund were considered part of the glacier (Raup and Khalsa 2007; Racoviteanu et al.
2 2009). Glacier area changes (1962 to 2000) and their dependency on topographic and
3 climatic variables were calculated on a glacier-by-glacier basis for the 232 glaciers in spatial
4 domain 2 using linear regression.

5 *3.4 Uncertainty estimates*

6
7 Glacier outlines derived from remote sensing data at various spatial and temporal
8 resolution are subject to various degrees of uncertainty, as discussed in recent studies
9 (Racoviteanu et al. 2009; Paul et al. 2013). This becomes an important issue in glacier change
10 analysis, where errors from various data sources accumulate at each processing step. The
11 main sources of uncertainty considered here are: 1) image classification errors (positional
12 errors and/or errors due to the semi-automated glacier mapping method); 2) conceptual errors
13 associated with the definition of a glacier, including mapping of ice divides, mixed pixels of
14 snow and clouds, and internal rock differences, which propagate to the glacier change
15 analysis, all described in detail in Racoviteanu et al. (2009).

16 (1) The errors in remote sensing glacier surface areas (E_{classif}) were estimated using the
17 “Perkal epsilon band” around each glacier outline dataset (Racoviteanu et al. 2009; Bolch et
18 al. 2010), using a ~1-pixel variability (Congalton 1991). Using ± 30 m for Landsat/ASTER,
19 ± 6 m for Corona and ± 3 m for QB outlines, the area uncertainty was $\pm 3\%$, $\pm 6\%$ and $\pm 2\%$ of
20 the glacierized area for Corona, Landsat/ASTER and QuickBird respectively. The Perkal
21 method is known to slightly over-estimate the errors, as described in Burrough and
22 McDonnel (1998). Recent glacier analysis comparison experiments reported a range of
23 uncertainty of $< 5\%$ for remote sensing glacier outlines compared to high-resolution imagery
24 (Raup et al. 2007; Paul et al. 2013). For manually-adjusted glacier outlines, particularly
25 debris-covered tongues, we used screen digitizing in streaming mode with a high density of

1 vertices to minimize area errors (B. Raup, National Snow and Ice Data Center, personal
2 communication, 2014).

3 (2) Uncertainties due to different digitization of internal rocks (E_{rocks}) were derived by
4 comparing area changes computed with internal rocks specific to each dataset, versus
5 “merged” internal rocks from each dataset. The differences in glacier datasets due to rock
6 inconsistencies amounted to $\sim 2\%$ of the glacier area. To minimize uncertainties in the glacier
7 area change, we merged rock outcrops from each dataset and removed them from all the area
8 calculations. The "inactive" bodies of ice above the bergschrund were included as part of the
9 glacier (Racoviteanu et al. 2009). For simplicity, we neglected the area change that might be
10 due to exposure of new internal rock due to glacier ice thinning.

11 Total errors in glacier area estimate for each dataset (E) were calculated as RMSE of the
13 classification (E_{classif}) and the internal rocks (E_{rock}):

$$E = \sqrt{E_{\text{classif}}^2 + E_{\text{rocks}}^2} \quad \text{Eq.1}$$

16 Errors in glacier surface area change (E_{change}) from 1962 to 2000 were computed as RMSE
18 of the total error for each time step calculated above (Eq.1):

$$E_{1962-2000} = \sqrt{E_{1962}^2 + E_{2000}^2} \quad \text{Eq.2}$$

21 **4. Results**

22 *4.1 The 2000 Landsat/ASTER glacier characteristics*

23

24 The 2000 glacier inventory based on Landsat and ASTER yielded 487 glaciers (of
25 which 162 were situated in Nepal, 186 in Sikkim, 30 in Bhutan and 109 in China), covering a
26 total surface area of $1463 \pm 88 \text{ km}^2$ (Table 4a). Of the 487 glaciers in this spatial domain, 68
27 glaciers (13%) had debris cover on their ablation areas. Supraglacial debris covered 160 ± 10
28 km^2 (11% of the glacierized area in spatial domain 1), with some differences between north

1 and south slopes of the study area, discussed later (section 5.1). In Sikkim, supraglacial
2 debris covered an area of $78 \pm 5 \text{ km}^2$ in 2000 (14% of the glacierized area).

3 ***[Table 4 a-b]***

4 In 2000, glacier size ranged from $0.02 - 105 \text{ km}^2$, with an average size of 3 km^2 and a
5 median size of 0.9 km^2 (Table 4b). The histogram of glacier area (Fig. 4a) is skewed to the
6 right (skewness = 8.4), showing that glaciers with area $< 10 \text{ km}^2$ are predominant in this
7 region, and glacier size decreases non-linearly. The long right-tail extremes represent only a
8 few glaciers such as Zemu, with an area $> 100 \text{ km}^2$.

9 ***[Fig. 4 a-d]***
10

11 The average slope of all glaciers in the inventory was 23 degrees, with a positive skew
12 (skewness = 0.38) (Fig. 4b) and no significant differences among the four regions ($p > 0.05$)
13 (Table 4b). Glacier length ranged from 0.08 km to 23 km (Zemu glacier), with an average of
14 2 km (Fig. 4c). Glacier thickness ranged from 3 m to 144 m, with the highest frequency for
15 thicknesses less than 30 m (Fig. 4d). The frequency distribution of both glacier length and
16 thickness were positively skewed, with long tails, indicating the prevalence of short, shallow
17 valley-type glaciers. Glacier aspect shows two predominant orientations: west-northwest (W-
18 NW) and east-northeast (E-NE), following the topographic divide (Fig. 5). On average,
19 glaciers on the Nepal side had an average aspect of 237 degrees (SW), whereas glaciers on
20 the Sikkim side had an average aspect of 131 degrees (SE), consistent with local topography.

21 ***[Fig. 5]***

22 Glacier termini elevations in the Landsat/ASTER domain ranged from 3,990 to 5,777 m,
23 with a mean of 4,908 m; median glacier elevation ranged from 4,515 to 6,388 m, with a mean
24 of 5,702 m (Table 4b). Considering glacier median elevation as a coarse approximation of
25 glacier equilibrium line altitude (ELA), our results are in agreement with Benn and Owen

1 (2005), who documented higher ELAs on the northern slopes of the Himalaya (6,000 – 6,200
2 m) compared to ELAs on the southern slopes (4,600 – 5,600 m).

3 4.2 Glacier area changes 1962 – 2000/2006 4

5 Overall, glaciers in the Corona spatial domain 2 lost $182.5 \pm 40 \text{ km}^2$ of their area (19
6 $\pm 7\%$, or $-0.5 \pm 0.2\% \text{ yr}^{-1}$) from 1962 to 2000 (Table 5). Overall, the average glacier area
7 changes were slightly smaller on the western side of the divide (Nepal, $16.9 \pm 4\%$ 1962 - 2000
8 or $0.44 \pm 0.2\% \text{ yr}^{-1}$) compared to the eastern side (Sikkim, $20.1 \pm 8\%$ 1962 – 2000 or $0.52 \pm$
9 $0.2\% \text{ yr}^{-1}$). When focusing on a smaller glacier subset in the Kanchenjunga-Sikkim subset
10 area (50 glaciers), we obtained an area change of $-10\% \pm 3\%$ ($-0.23 \pm 0.08\% \text{ yr}^{-1}$) based on
11 high-resolution imagery (1962 to 2006) (Table 5). The rates of glacier area change for this
12 group are overall 50% lower than the rates of change in the larger spatial domain 1 perhaps
13 due to higher percentage of debris (21 %) compared to the entire Landsat/ASTER spatial
14 domain 2 (11%).

15 [Table 5]

16 On a glacier-by-glacier basis, glaciers in the Corona domain lost 2% to 95 % of their
17 area, with a mean of 32% from 1962 to 2000 (Fig. 6). The spatial distribution of these area
18 changes, illustrated in Fig. 6, shows that the largest area changes ($> 70\%$ area loss) occurred
19 for only a few isolated glaciers in the northern and southern extremities of the study area (17
20 glaciers). A closer examination of these glaciers revealed that these were small clean glaciers
21 ($< 0.1 \text{ km}^2$), with steep slopes (mean of 26 degrees), posing a need to investigate the
22 topographic controls on area change, and clean vs. debris-covered glaciers separately.

23 [Fig. 6]

24 Clean glaciers lost more of their area from 1962 to 2000 (34%) compared to debris-
25 covered glaciers (22 %) across the region, with little differences east-west (Nepal and

1 Sikkim)(Table 6). The difference in mean rates of area change between clean and debris
2 covered glaciers was statistically significant based on two-sample F-test (p-value < 0.05).

3 **[Table 6]**

4 Fig. 7a-b, shows a larger spread and a higher percentage of surface area loss of clean
5 glaciers compared to debris-covered glaciers. For both glacier types, however, there is a high
6 variability in percent area change, perhaps due to other factors such as local topography.

7 **[Fig. 7 a-b]**

8 Linear regression analysis showed that percent area change per glacier was negatively
9 correlated to glacier area, altitudinal range, glacier elevation (median and maximum elevation
10 and aspect (significant correlations at 99% confidence interval, $p < 0.01$) (Table 7). Glacier
11 minimum elevation and slope were significant controls on glacier area change at 95%
12 confidence interval ($p < 0.05$). Solar radiation, precipitation and percent debris were not
13 statistically significant controls on glacier area change ($p > 0.1$, confidence interval 90%)
14 (Table 7). These are discussed in section 5.3.

15 **[Table 7]**

16 Clean and debris-covered glaciers showed significant differences in terms of glacier area,
17 area change, minimum elevation, altitudinal range and length based on a two sample F-test
18 for variances) ($p < 0.05$) (Table 8). Clean glaciers in this area are ~12 times smaller (1 km²
19 on average) than debris-covered glaciers (15 km²), they have higher termini elevations (+ 391
20 m), and an overall altitudinal range about 3 times smaller than debris-covered glaciers (Table
21 7). On a glacier-by-glacier basis, clean glaciers lost more area (34 %) than debris covered
22 glaciers (22%) from 1962 to 2000. Clean glaciers with smaller altitudinal range tend to
23 display more area loss compared to debris-covered glaciers.

24 **[Table 8]**

25

1 **5. Discussion**

2 *5.1 Spatial distribution of glacier characteristics across the study area*

3 One of the important steps in utilizing our glacier inventory data is to understand spatial
4 patterns in glacier characteristics across the region. Our study area displays region-wide
5 consistency in glacier characteristics notably glacier area, elevation and topography across
6 four sub-regions based on the 2000 glacier data (Table 4). For example, the prevalence of
7 small glaciers noted in this area is consistent with worldwide patterns, also observed for the
8 Cordillera Blanca of Peru in a previous study (Racoviteanu et al, 2008a). There is variability
9 within eastern Himalaya, for example the mean glacier size reported in this study area (3
10 km²) is double compared to Khumbu region, west of our study area (1.4 km²) (Bajracharya
11 and Shrestha 2011). The glacier slope across our study area (23 degrees) is consistent with
12 average glacier slopes reported for the Khumbu region in Nepal (22 degrees) (Salerno et al.
13 2008; Bajracharya and Shrestha 2011), indicating a general tendency for steep glaciers across
14 the region. There are only a few large, long glaciers in the area such as Zemu glacier (103
15 km², 23 km in 2000). With respect to glacier aspect, we also note similar predominant
16 orientations of glaciers southwards, in the direction of the prevailing monsoon circulation
17 consistent with other studies such as the Khumbu region (average aspect 181 degrees) (Mool
18 et al. 2002; Salerno et al. 2008).

19 The comparison of glacier characteristics across sub-regions points to a pronounced
20 gradient north to south (Bhutan/China sub-regions compared to Sikkim/Nepal), particularly
21 with respect to glacier elevations and debris cover. Glaciers on northern side of the divide
22 (China) have higher glacier termini and median elevations compared to the southern side
23 (Nepal and Sikkim) (+700 m and +400 m respectively) (Table 4). These differences seem to
24 be consistent with general air circulation patterns in the area. The Asian summer monsoon
25 brings large amounts of precipitation on the southern slopes of the Himalaya, favoring glacier

1 growth at lower elevations and a lower ELA. In contrast, in the upper reaches of the valleys
2 and on the Tibetan plateau, the monsoon is blocked by the topographic barrier (Clift and
3 Plumb 2008), causing a drier climate and higher glacier ELAs. There is a much less
4 pronounced east-west gradient in glacier elevations, with higher glacier minimum and
5 median elevations on the western side (Nepal) (+50 m) compared to the eastern side
6 (Sikkim). This may be explained by the location of Nepalese glaciers on the western side of
7 the topographic divide, away from the prevailing monsoon.

8 Debris coverage also shows a pronounced variability north to south of the topographic
9 divide. Himalayan glaciers are often referred to as “heavily” debris-covered, but the percent
10 glacierized area covered by supra-glacial debris cover varies across the mountain range. In
11 our study area, debris cover is more prevalent on the southern side of the divide (Sikkim,
12 14% of glacierized area) compared to the northern one (China, 2% of the glacierized area),
13 perhaps due to different geologic and topographic patterns. The northern side of the divide,
14 which is part of the Tibetan plateau, is situated in a monsoon shadow and is therefore dry; the
15 gentler slopes induce lower rates of erosion. In contrast, the southern slopes of the Himalaya
16 tend to be heavily covered with debris cover due to the abundance of rock material from the
17 steep slopes. The steep slopes made of soft sedimentary rocks and Precambrian crystalline
18 rocks (Mool et al. 2002) and are prone to high rates of erosion, particularly with large
19 amounts of monsoon moisture. This north-south difference in debris cover amount was also
20 noted in other studies (Scherler et al. 2011). In our study, we found a lower percent of debris
21 coverage (21%) than the entire central/eastern Himalaya reported in Scherler et al. (2011)
22 (36% debris cover), or from the Khumbu region, west of our study area, by Fujii and Higuchi
23 (1977), Nuimura et al. (2012) (34.8%), Racoviteanu et al. (2013a) (27 %) and Thakuri et al.
24 (2014) (32%).

25

5.2 Regional glacier area changes

The overall rate of surface area loss of $0.5 \pm 0.2\% \text{ yr}^{-1}$ from 1962 to 2000 for Sikkim and eastern Nepal obtained here is in agreement with other studies from the southern slopes of the Himalaya. Similar rates of area loss (0.1 to $0.3\% \text{ yr}^{-1}$) were reported from the Khumbu and Garwhal regions, west of our study area, for approximately the same time period (Bolch et al. 2008a; Bhambri et al. 2011; Nuimura et al. 2012; Basnett et al. 2013; Thakuri et al. 2014). Similarly, for glaciers of Bhutan, east of our study area, Karma et al. (2003) found an average surface glacier area loss of $0.3\% \text{ yr}^{-1}$ from 1963 to 1993. It is worth mentioning that these rates of area change are lower than those previously reported for the drier monsoon-transition zone in the western Himalaya ($0.7\% \text{ yr}^{-1}$) by Kulkarni et al. (2007), which raised concerns about the future of Himalayan glaciers. In a more recent study, Bahuguna et al. (2014) found lower rates of glacier area loss ($0.4\% \text{ yr}^{-1}$) for the same area (Himachal Pradesh in the western Himalaya), which is in agreement with rates of area loss we report here for eastern part. Updated glacier area changes from recent studies (Bolch et al. 2012; Bahuguna et al. 2014; Racoviteanu et al. 2014) also point at lower rates of area loss than previously reported, particularly for the Indian Himalaya. The similar overall rate of glacier area change in the eastern part compared to western one for both debris covered glaciers and clean glacier types suggest consistent patterns across the region (Table 5).

The smaller glacier area loss for debris-covered glaciers noted in our study is in agreement with studies from Khumbu (Nuimura et al. 2012; Thakuri et al. 2014) or other studies in the central-eastern Himalaya (Bolch et al. 2008a; Bhambri et al. 2011; Thakuri et al. 2014). These studies also reported lower rates of glacier surface area loss and even stable or less retreating glacier termini for debris-covered tongues compared to clean glaciers (Scherler et al. 2011). Area changes for debris-covered glaciers need to be interpreted with caution, due to the wide variability in debris cover characteristics such as thickness.

1 Furthermore, these stagnating or less changing tongues may not reflect the true state of the
2 glaciers, for example patterns of glacier thinning, which may occur at similar rates to clean
3 glaciers (Gardelle et al. 2012a; Kääb et al. 2012).

4

5 *5.3 Topographic and climatic controls on area changes*

6 While the consistent area change patterns across the sub-regions (east to west) are useful
7 for comparison with larger areas, these patterns cannot be used to understand glacier-by-
8 glacier variability in area changes, which may be controlled by local topography and climate.
9 In this study, we found that topographic factors, notably glacier size, glacier altitude
10 (maximum, median, altitudinal range) and aspect were most important in determining rates of
11 glacier area loss in spatial domain 1. Glacier size plays a significant role in determining area
12 change, i.e. smaller glaciers experienced higher rates of area loss (Table 7). The tendency of
13 larger glaciers to lose less area ($>20 \text{ km}^2$) was observed in various studies (Racoviteanu et al.
14 2008a; Salerno et al. 2008; Loibl et al. 2014), though in the case of Salerno et al. (2008), for
15 the Khumbu, the correlation was not statistically significant. Higher glacier elevations and
16 larger altitudinal ranges significantly reduce the rates of area loss, as was also noted in the
17 Khumbu region in Nepal and elsewhere (Bolch et al. 2008a; Scherler et al. 2011; Loibl et al.
18 2014; Thakuri et al. 2014). The dependency of area change on glacier size and elevation is
19 also consistent with observations from the Cordillera Blanca of Peru (Racoviteanu et al.
20 2008a) in the outer tropics, indicating consistent patterns in glacier area changes worldwide.

21

[Table 7]

22 Glacier slope also plays a significant role in determining glacier area change, i.e. the
23 steeper the glacier, the larger the area loss observed in our study. The same tendency was
24 observed in the Khumbu area (Salerno et al. 2008), but the correlation is less significant than
25 the glacier altitude ($p < 0.05$). The presence of gentle slopes covered with supra-glacial debris

1 in the ablation areas of glaciers, fairly common in this area, may have reduced the strength of
2 the correlation. Glacier aspect was also found to be a significant control on area change, with
3 more area loss for glaciers oriented southwards and south-west ($p < 0.01$). This is in agreement
4 with findings from Salerno et al. (2008) for the Khumbu region, but is in contrast with results
5 from Loibl et al. (2014) for the Nyainqêntanglha Range in southeastern Tibet, about 600 km
6 east of our study area, who found that south-facing glaciers experienced smaller rates of
7 terminus retreat. Percent debris cover was a negative control on area change, i.e. glaciers with
8 more extensive debris cover on their areas tend to lose less area overall, but this was not
9 statistically significant ($p > 0.05$). Debris covered glaciers may benefit from the insulating
10 effect of debris cover above a certain “critical” debris thickness (Mihalcea et al. 2008a;
11 Zhang et al. 2011), which needs to be further investigated.

12 Geographic location (latitude and longitude) were negative controls on glacier area change
13 suggesting that glaciers located north and eastwards of the study area tend to lose more area,
14 but only latitude was statistically significant ($p < 0.05$). Climate indices (precipitation and
15 solar radiation) were not significant factors controlling glacier area loss. In contrast, Loibl et
16 al. (2014) showed that glaciers located in a monsoon-influenced area were more sensitive to
17 climate change. This is in agreement with larger-scale studies (Gardelle et al. 2013), which
18 indicated a tendency for enhanced glacier wastage in the eastern, monsoon-influenced parts
19 of the Himalaya. With respect to climatic factors in this area, Basnett et al. (2013) reported an
20 increase in mean annual temperature, more significantly in the winter ($+2^{\circ}\text{C yr}^{-1}$ in the last
21 four decades). Increasing temperatures on the south slopes of the Himalayas were also noted
22 in other studies (Shrestha et al. 2000; Thakuri et al. 2014) based on instrumental data, but
23 were estimated to have less effect on glacier area than changes in precipitation because of the
24 orientation of these glaciers towards the prevailing monsoon circulation. In our study, the
25 climatic control on glacier area is not conclusive, and finer-resolution, more accurate

1 temperature and precipitation datasets would be needed. Furthermore, similarly to areas
2 further east (Loibl et al. 2014), average annual solar radiation and latitude were not found to
3 be significant controls on glacier area change in our study.

4

5 *5.4 Surface temperature distribution on debris cover tongues*

6 Smaller rates of area change for the debris-covered glaciers may be further explained by
7 surface characteristics of debris cover (thickness, thermal conductivity and resistance).
8 However, these are not easily available in this area due to the lack of field-based
9 measurements, and the difficulty of conducting surveys on the debris-covered tongues.
10 Therefore, in this study, we are qualitatively showing the distribution of surface temperature
11 on selected debris-covered tongues in spatial domain 3 based on the 2002 ASTER scene. Fig.
12 8 shows a high variability in supra-glacial surface temperature at 90 m spatial resolution, but
13 there is no clear general temperature trend for the eastern slopes (Sikkim side) versus the
14 western slopes (Nepal) side. The fluctuations in surface temperatures along transects are
15 clearly visible on Fig. 9, with some sharp spikes of high and low temperatures, particularly
16 for Kanchenjunga and Yalung glaciers (labeled “A” and “B” on Fig. 8). This strong
17 variability in supraglacier debris temperatures may be due to the presence of surface features
18 such as debris thickness, size of the debris particles, and thermal resistance and conductivity
19 of the debris. For the debris-covered tongues investigated here, the supraglacier temperatures
20 range from 0°C to 30°C, suggesting that the supra-glacier debris heats up considerably during
21 the day. At the glacier scale, temperature drops over supra-glacial features such as ice walls
22 and supra-glacial lakes, which tend to be colder than the surrounding debris, and this is
23 visible even at the coarse spatial resolution of the temperature data (90 m). On Fig. 9 we note
24 the slight upward trend for supra-glacier temperature towards the glacier termini, particularly
25 for Zemu glacier (“C” on Fig. 8). For this glacier, the middle-upper part of the debris surface

1 is colder (-3 to 5°C) than the last 10 km towards the glacier terminus (5 to 14°C) (Fig. 9). In a
2 different paper (Racoviteanu and Williams, 2012), we found similar patterns of surface
3 temperature increasing towards the glacier terminus for the same glacier, but based on a
4 different scene (November 2001), indicating consistent patterns for this glacier. The higher
5 surface temperatures towards the glacier terminus may indicate a thicker debris cover, which
6 insulates the ice underneath, noted on other studies (Mihalcea et al. 2008a). The day-time
7 debris temperature ranges and the strong spatial variability noted here are similar to the ones
8 we found for Khumbu, west of this study area (-3 to 17°C) (Racoviteanu et al. 2013b). In
9 Khumbu, we found that supra-glacier debris had a distinct temperature signal compared to
10 other surfaces such as non-ice moraine, clean ice, and supra-glacier/pro-glacier lakes, with
11 more pronounced differences among these three during the daytime.

12 *[Fig. 8 and 9]*

13 The suitability of ASTER-based surface for inferring debris characteristics, most notably
14 thickness, has been demonstrated in other studies (Suzuki et al. 2007; Mihalcea et al. 2008a;
15 Zhang et al. 2011). For this study area, there were no field measurements available to test the
16 validity of ASTER temperatures for quantifying supra-glacier debris characteristics.
17 However, in a different study (Racoviteanu et al. 2013b), we validated ASTER-based surface
18 temperatures extracted from 9 night scenes from 2010 – 2011 for the Khumbu by inverting
19 field-based long-wave radiation (L_{out}) using the Stefan-Boltzmann law ($L_{out} = \epsilon T^4$). The
20 measurements were from the automatic weather station (AWS) installed on Changri Nup
21 glacier (Wagnon et al. 2013). We found a good agreement between ASTER temperatures and
22 field-based measurements ($R^2 = 0.92$) using a sensitivity analysis ($\epsilon = 0.97 \pm 0.1$) to account
23 for small-scale variability in emissivity. Given that the Kanchenjunga-Sikkim area has
24 similar characteristics to Khumbu in terms of debris cover, geographic location, and that the

1 images were acquired around the same time of the year as the Khumbu (Nov.- Jan.), we
2 consider that this validation may be applicable to the present study area.

3 *5.4 The role of glacier lakes*

4 The role of supra-glacier/pro-glacier lakes for glacier area change in this area of the
5 Himalaya was addressed in detail in recent studies (Basnett et al. 2013; Bajracharya et al.
6 2014). Gardelle et al. (2011) also pointed out the increased formation of supra-glacier lakes
7 particularly for the eastern part of the Himalaya. A quantitative assessment of lake formation
8 is beyond the scope of this paper; here we only illustrate qualitatively some of the changes
9 occurring on glaciers with supra-glacial or pro-glacial lakes using high-resolution Corona and
10 QuickBird imagery. For the Tista basin in Sikkim, Mool and Bajracharya (2003) inventoried
11 266 glacier lakes covering a total area of 20 km² (3.5% of the glacierized area) based on 2000
12 Landsat ETM+ imagery. For spatial domain 3, we estimated that glacier lakes covered 1.3%
13 of the total debris-covered glacier area, or 5.8% of the area if we consider only the debris-
14 cover (ablation) part, based on the QB/WV2 imagery. Salerno et al. (2012) reported similar
15 percentage for the area of supraglacial lakes, i.e. (0.3 – 2% of the overall glacierized area) for
16 the Khumbu region. While supra-glacier lakes do not cover extensive areas of the glacierized
17 surface, they were shown to increase surface ablation rates in this part of the Himalaya (Sakai
18 et al. 2002; Fujita and Sakai 2014). It was also shown that supra-glacier lakes located at the
19 glacier terminus tend to merge to create large, fast growing pro-glacier lakes which accelerate
20 glacier area loss (Basnett et al. 2013; Bajracharya et al. 2014).

21 Some of the pro-glacier lakes in our study area are visible on Fig. 10 and 11 for the
22 northern part of spatial domain 3 (Changsang, East Langpo, Jongsang, Middle Lhonak, South
23 Lhonak). Most of these lakes are moraine-dammed lakes, considered dangerous for
24 potentially inducing glacier lake outburst flood events, and were shown to accelerate the
25 glacier area loss in the recent decades (Bajracharya et al. 2014). Fig.10 a-b shows the

1 evolution of the pro-glacier lake on N. and S. Lhonak glaciers in Sikkim, also noted in
2 Basnett et al. (2013). A closer look at a subset area (Fig. 11) shows the visible growth of a
3 pro-glacial lake for the adjacent N. Lhonak and S. Lhonak glaciers. We estimate that these
4 two glaciers retreated ~650 m and 1.3 km from 1962 to 2006, respectively. Another branch of
5 N. Lhonak glacier has wasted significantly by ~1.5 km from 1962 to 2006, and a glacier
6 outlet is now clearly visible. The northern branch of Jongsang glacier was entirely covered by
7 a supra-glacier lake in 2006, while another part shows less significant rates of terminus
8 retreat (~100 m in 44 years). A part of the Jongsang glacier shows a slight “false” glacier
9 tongue advance due to uncertainties in the mapping of Corona imagery. While our purpose
10 here is not to present glacier length changes, we note that these estimates are in agreement
11 with trends of glacier thinning and increased glacier lake formation reported in this area of
12 the Himalaya previously (Gardelle et al. 2011; Kääb et al. 2012; Basnett et al. 2013).

13 *[Fig. 10 and 11]*

14 *5.5 Uncertainty and limitations*

15 Inconsistencies in glacier area change estimates have been pointed out in other
16 studies, for the Himalaya and elsewhere (Racoviteanu et al. 2008a; Racoviteanu et al. 2008b),
17 and are also noted in the current study. Glacier area changes in the Himalaya are
18 heterogeneous, and depend on a variety of factors including local topography and climate, so
19 some caution should be applied when comparing rates of area changes from one area to other
20 areas, even in the same climatic zone. For example, for Sikkim, we estimated a surface area
21 change of $-88.9 \pm 5 \text{ km}^2$ (-13.5% from 1962 to 2006, or $-0.36 \pm 0.17 \text{ \% yr}^{-1}$). Other studies in
22 this area point to contrasting results. For the same geographic area, Basnett et al. (2013)
23 reported an area change of $-0.16 \pm 0.10 \text{ \% yr}^{-1}$ from 1989/1990 to 2009/2010), which about
24 half of the area change in our findings. In contrast, a recent study (Bahuguna et al. 2014)
25 reported the highest rates of area change (about -0.8% yr^{-1}) for the last decade, even higher

1 than rates reported previously for the western Himalaya by Kulkarni et al. (2007). We
2 speculate that such large differences might be due to errors inherent in the baseline datasets,
3 coupled with misclassification due to snow cover or debris-covered areas.

4 Glacier area changes reported for Sikkim in different studies, using a variety of data,
5 including topographic maps (Table 9), illustrates this point. For example, for Sikkim, our
6 study estimated $569 \text{ km}^2 \pm 70 \text{ km}^2$ of glacierized area in 2000 based on Landsat/ASTER data.
7 For the same time period, Mool et al. (2002) reported an area of 577 km^2 based on the same
8 source imagery (Landsat ETM+) (Table 9). These two area estimates differ only by 8.2 km^2
9 (1.4%) of our estimated area, only the number of glacier differs substantially (186 glaciers in
10 our study compared to 285 glaciers in ICIMOD study), most likely due to the way in which
11 ice masses were split and how glaciers were counted. Methodology differences and
12 inconsistencies in glacier estimates are quite common in multi-temporal image analysis
13 performed by different analysts, and were previously noted in other areas of the world
14 (Racoviteanu et al. 2009). Similarly, for the 1962 decade, our analysis of Corona 1962
15 imagery for Sikkim yielded 178 glaciers with an area of $658 \pm 20 \text{ km}^2$. In a recent publication
16 (Racoviteanu et al. 2014), we reported 158 glaciers with an area of 742 km^2 for the 1960s
17 based on the Swiss topographic map. The Geological Survey of India (GSI) (Sangewar and
18 Shukla 2009) reported 449 glaciers with an area of 706 km^2 for the 1970s based on
19 topographic maps. Our 1962 Corona glacier inventory yields a smaller total glacier area than
20 the one based on the topographic map (84 km^2 , or 11%) (Racoviteanu et al. 2014) or the GSI
21 inventory based on topographic maps (48.3 km^2 , or 7 % area) (Sangewar and Shukla 2009).
22 We consider that both of these mentioned studies overestimated the glacier area in the 1960s,
23 perhaps due to the presence of persistent snow in the source aerial imagery.

24 Subsequent glacier inventories in Sikkim also point to contradictory patterns. For the
25 1980s, another study (Kulkarni 1992b) reported a glacierized area of 431 km^2 for 1987/1989

1 based on Indian IRS-1A and Landsat data. Considering our 1962 Corona inventory, this
2 would imply an area loss of 42% since 1962 ($2.1\% \text{ yr}^{-1}$), followed by a strong increase in
3 glacier area ($+33.5\%$, or $+3\% \text{ yr}^{-1}$) from 1987/1988 to 2000 (based on our Landsat analysis),
4 which is undocumented in this area. We consider the 1987/89 estimates to be highly
5 unreliable, given that there are no glacier surges that might induce an apparent “glacier
6 growth”. In some areas, we noted omissions of some debris-covered tongues from the glacier
7 maps, which might explain some of the differences. We consider the Corona 1962 dataset to
8 be more reliable than the inventories based on topographic maps, and hence we used this
9 dataset as baseline for comparison with the recent imagery.

10 *[Table 9]*

11 **6. Summary and outlook**

12
13 In this study we combined remote sensing data from various sensors to construct a new
14 glacier inventory for the Kanchenjunga-Sikkim region in the eastern Himalaya. Based on
15 1962 Corona and 2006 QuickBird imagery, we found an overall negative glacier surface area
16 change of $0.5 \pm 0.2\% \text{ yr}^{-1}$ since 1962, in agreement with those noted in other studies in the
17 Himalaya. The area change rates reported here are lower than the average rate of $-0.7\% \text{ yr}^{-1}$
18 reported in other glacierized areas of the world such as the Alps (Kääb et al. 2002), the Tien
19 Shan (Bolch 2007) and the Peruvian Andes (Racoviteanu et al. 2008a). Glaciers exhibit
20 heterogeneous patterns of area change, depending on topographic and climatic factors, more
21 notably glacier altitude (maximum, median, altitudinal range), glacier size, slope and aspect.
22 Glacier area changes depend strongly on glacier size and elevation, which is consistent with
23 other areas in the central-eastern Himalaya (Thakuri et al. 2014) or elsewhere, for example
24 the outer tropics (Racoviteanu et al. 2008a). The conclusions drawn with respect to spatial

1 patterns in glacier characteristics, glacier area loss, and their topographic and climatic
2 dependency, include:

- 3 • We found a strong north-south gradient in terms of glacier elevations and debris
4 cover, with larger percent of area covered by debris, and higher glacier elevations
5 on the northern side for the divide, but less east to west gradient in these
6 characteristics;
- 7 • Glacier area change (loss) of $0.5 \% \pm 0.2\% \text{ yr}^{-1}$ from 1962 to 2000, with some
8 differences on the eastern side of the divide (Sikkim, $-0.52 \% \pm 0.2\% \text{ yr}^{-1}$) versus
9 the western part (Nepal, $-0.44 \% \pm 0.2\% \text{ yr}^{-1}$);
- 10 • Higher rates of area loss for clean glaciers (-34% , or $-0.7\% \text{ yr}^{-1}$) compared to
11 debris-covered glaciers (-14.3% or -0.3 yr^{-1}) across the sub-regions on a glacier-by-
12 glacier basis;
- 13 • The amount of glacier area loss is partly controlled by a glacier's headwater
14 elevation, altitudinal range, glacier area, slope and aspect, with the largest area loss
15 observed for small, steep glaciers with a smaller altitudinal range and less debris
16 cover;
- 17 • Supra-glacial debris cover is prevalent on the southern slopes of the Himalaya
18 (14% of the glacierized area) compared to northern slopes (2%);
- 19 • Supraglacial lakes constitute about 6% of the debris covered area, and some of
20 these supra-glacial lakes have merged to form pro-glacial lakes;
- 21 • While Himalayan glaciers are undoubtedly undergoing negative area change, the
22 rates of area loss noted in this study ($0.5\% \text{ yr}^{-1}$) as well as other recent studies in
23 the area ($0.2 - 0.4\% \text{ yr}^{-1}$ since the 1960s) are lower than other glacierized areas
24 worldwide ($0.7\% \text{ yr}^{-1}$).

25 The glacier area change estimates reported here are subject to uncertainties, most

1 notably with respect to early topographic maps and declassified Corona imagery, therefore a
2 considerable effort was given to minimizing errors by multiple re-iterations of the glacier
3 outlines. The understanding of the spatial patterns of glacier changes in the current study is
4 limited by: 1) a lack of a baseline elevation dataset for the 1960 to compute glacier elevation
5 changes from 1960s to 2000; 2) lack of field-based measurements to validate debris-cover
6 mapping and surface temperature distribution. With respect to the latter, while surface
7 temperature trends show a slight increase towards the terminus, suggesting a thicker debris
8 cover, the supra-glacial surface temperatures are highly heterogenous and require additional
9 investigation. A further improvement in the current study will be to include the supra-glacial
10 and pro-glacial lakes and surface temperature as determinant factors for the glacier area
11 change, perhaps in a more sophisticated multivariate regression model. The glacier datasets
12 constructed in this study can be further utilized to understand the behavior of glaciers in this
13 little-investigated area of the Himalaya, particularly with respect to spatial patterns of glacier
14 melt, and the contribution of glaciers to water resources.

15 **Acknowledgements**

17 This research was funded by a NASA Earth System Sciences (ESS) fellowship
18 (NNX06AF66H), a National Science Foundation doctoral dissertation improvement grant
19 (NSF DDRI award BC 0728075), a CIRES research fellowship, and a graduate fellowship
20 from CU-Boulder. A. Racoviteanu's post-doctoral research was funded by Centre National
21 d'Etudes Spatiales (CNES), France. Participation of M. Williams was supported by the NSF-
22 funded Niwot Ridge Long-Term Ecological Research (LTER) program and the USAID
23 Cooperative Agreement AID-OAA-A-11-00045. ASTER imagery was obtained through the
24 NASA-funded Global Land Ice Measurements from Space (GLIMS) project. We are grateful
25 to Jonathan Taylor at University of California-Fullerton for facilitating access to high-
26

1 resolution imagery through the NASA Appropriations Grant # NNA07CN68G. We thank Dr.
2 Damodar Lamsal and an anonymous reviewer for their thorough comments, which helped
3 improve the manuscript.

4

5

6 **References:**

7

8

9

10 Ageta, Y. and Higuchi, K. (1984). "Estimation of Mass Balance Components of a Summer-
11 Accumulation Type Glacier in the Nepal Himalaya." *Geografiska Annaler Series a-Physical*
12 *Geography* **66**(3): 249-255.

13

14

15 Andermann, C., Bonnet, S. and Gloaguen, R. (2011). "Evaluation of precipitation data sets
16 along the Himalayan front." *Geochemistry, Geophysics, Geosystems* **12**(7): Q07023.
17 10.1029/2011gc003513.

18

19

20 Andreassen, L. M., F. paul, A. kääb and J. e. hausberg (2008). "The new Landsat-derived
21 glacier inventory for Jotunheimen, Norway, and deduced glacier changes since the 1930s."
22 *Cryosphere Discuss* **2**: 299 - 339.

23

24

25 Bahuguna, I. M., A.V. Kulkarni, M. L. Arrawatia and D. G. Shresta (2001). *Glacier Atlas of*
26 *Tista Basin (Sikkim Himalaya)*. Ahmedabad, India: SAC/RESA/MWRGGLI/SN/16.

27

28

29 Bahuguna, I. M., B. P. Rathore¹, Brahmabhatt, R., Sharma, M., Dhar, S., Randhawa, S. S.,
30 Kumar, K., Romshoo, S., Shah, R. D. and Ganjoo, R. K. (2014). "Are the Himalayan glaciers
31 retreating?" *Curr Sci* **106**: 1008 - 1013.

32

33

34 Bajracharya, S. R., Maharjan, S. B. and Shresta, F. (2014). "The status and decadal change of
35 glaciers in Bhutan from 1980's to 2010 based on the satellite data." *Annals of Glaciology*
36 **55**(66): 159 - 166. doi: 10.3189/2014AoG66A125, 2014.

37

38

39 Bajracharya, S. R., Mool, P. K. and Shresta, A. (2007). *Impact of climate change on*
40 *Himalayan glaciers and glacial lakes*. ICIMOD, Kathmandu, pp.

41

42

43 Bajracharya, S. R. and Shrestha, B., Eds. (2011). The status of glaciers in the Hindu-Kush
44 Himalayan Region. Kathmandu, Nepal, International Centre for Integrated Mountain
45 Development (ICIMOD). 127 pp.

46

1
2 Basnett, S., Kulkarni, A. and Bolch, T. (2013). "The influence of debris cover and glacial
3 lakes on the recession of glaciers in Sikkim Himalaya, India." *Journal of Glaciology* **59**(218):
4 1035 - 1046.
5
6
7 Benn, D. and Owen, L. A. (2005). "Equilibrium-line altitudes of the Last Glacial Maximum
8 for the Himalaya and Tibet: an assessment and evaluation of results." *Quaternary Int* **138** -
9 **139**: 55 -58.
10
11
12 Benn, D. I. and Owen, L. A. (1998). "The role of the Indian summer monsoon and the mid-
13 latitude westerlies in Himalayan glaciation: review and speculative discussion." *Journal of*
14 *the Geological Society* **155**(2): 353-363.
15
16
17 Berthier, E., Arnaud, Y., Kumar, R., Ahmad, S., Wagnon, P. and Chevallier, P. (2007).
18 "Remote sensing estimates of glacier mass balances in the Himachal Pradesh (Western
19 Himalaya, India)." *Remote Sensing of Environment* **108**(3): 327 - 338.
20
21
22 Berthier, E., Arnaud, Y., Vincent, C. and Remy, F. (2006). "Biases of SRTM in high-
23 mountain areas: Implications for the monitoring of glacier volume changes." *Geoph Res Lett*
24 **33**(8): L08502. doi:08510.01029/ 02006GL025862.
25
26
27 Bhambri, R. and Bolch, T. (2009a). "Glacier mapping: a review with special reference to the
28 Indian Himalayas." *Progr Phys Geogr* **33**(5): 672 - 702.
29
30
31 Bhambri, R., Bolch, T., Chaujar, R. K. and Kulshreshth, S. C. (2010). "Glacier changes in the
32 Garhwal Himalayas, India during the last 40 years based on remote sensing data." *Journal of*
33 *Glaciology* **54**(203): 543 - 556.
34
35
36 Bhambri, R., Bolch, T., Chaujar, R. K. and Kulshreshtha, S. C. (2011). "Glacier changes in
37 the Garhwal Himalaya, India, from 1968 to 2006 based on remote sensing." *Journal of*
38 *Glaciology* **57**(203): 543 - 556.
39
40
41 Bhatt, B. C. and Nakamura, K. (2005). "Characteristics of Monsoon rainfall around the
42 Himalayas revealed by TRMM precipitation radar." *Monthly Weather Review* **133**: 149 -
43 165. <http://dx.doi.org/10.1175/MWR-2846.1>.
44
45
46 Bolch, T. (2007). "Climate change and glacier retreat in northern Tien Shan
47 (Kazakhstan/Kyrgyzstan) using remote sensing data." *Global Planet Change* **56**(1-2): 1-12.
48
49

1 Bolch, T., Buchroithner, M. F., Pieczonka, T. and Kunert, A. (2008a). "Planimetric and
2 Volumetric Glacier Changes in the Khumbu Himalaya since 1962 Using Corona, Landsat
3 TM and ASTER Data." *J Glaciol* **54**(187): 592 - 600.
4
5
6 Bolch, T., Kulkarni, A., Käab, A., Huggel, C., Paul, F., Cogley, J. G., Frey, H., Kargel, J. S.,
7 Fujita, K., Scheel, M., Bajracharya, S. and Stoffel, M. (2012). "The State and Fate of
8 Himalayan Glaciers." *Science* **336**(6079): 310-314. 10.1126/science.1215828.
9
10
11 Bolch, T., M.F.Buchroithner, J.Peters, M.Baessler and Bajracharya, S. (2008b).
12 "Identification of glacier motion and potentially dangerous glacial lakes in the Mt. Everest
13 region/Nepal using spaceborne imagery." *Nat.Hazards Earth Syst. Sci* **8**: 1329 - 1340.
14
15
16 Bolch, T., Menounos, B. and Wheate, R. (2010). "Landsat-based inventory of glaciers in
17 western Canada, 1985–2005." *Remote Sensing of Environment* **114**(1): 127 - 137.
18
19
20 Bolch, T., Pieczonka, T. and Benn, D. I. (2011). "Multi-decadal mass loss of glaciers in the
21 Everest area (Nepal Himalaya) derived from stereo imagery." *The Cryosphere* **5**(2): 349-358.
22 10.5194/tc-5-349-2011.
23
24
25 Bookhagen, B. and Burbank, D. W. (2006). "Topography, relief and TRMM-derived rainfall
26 variations along the Himalaya." *Geoph Res Lett* **33**(L08405): doi::10.1029/2006gl026037.
27
28
29 Burrough, P. A. and Mcdonnel, R. A. (1998). *Principles of Geographic Information Systems.*,
30 Oxford University Press.
31
32
33 Cgiar-Csi (2004). "Void-filled seamless SRTM data V1." International Centre for Tropical
34 Agriculture (CIAT), available from the CGIAR-CSI SRTM 90m Database:
35 <http://srtm.csi.cgiar.org> and <http://www.ambiotek.com/topoview>. Last accessed: 2014-04-
36 01.
37
38
39 Clift, P. D. and Plumb, R. A. (2008). *The Asian Monsoon: Causes, History and Effects.* New
40 York, Cambridge University Press.
41
42
43 Congalton, R. G. (1991). "A review of assessing the accuracy of classifications of remotely
44 sensed data." *Rem Sens Environ* **37**: 35 - 46.
45
46
47 Dashora, A., Lohani, B. and Malik, J. N. (2007). "A repository of Earth resource information-
48 CORONA satellite programme." *Current Science* **92**(7): 926 - 932.
49
50

1 Digital_Globe (2007). "QuickBird Imagery Products- Product Guide. Revision 4.7.3." Last
2 accessed: 08-15, 2011, from
3 [http://www.hatfieldgroup.com/UserFiles/File/GISRemoteSensing/ResellerInfo/QuickBird/Qu](http://www.hatfieldgroup.com/UserFiles/File/GISRemoteSensing/ResellerInfo/QuickBird/QuickBird%20Imagery%20Products%20-%20Product%20Guide.pdf)
4 [ickBird%20Imagery%20Products%20-%20Product%20Guide.pdf](http://www.hatfieldgroup.com/UserFiles/File/GISRemoteSensing/ResellerInfo/QuickBird/QuickBird%20Imagery%20Products%20-%20Product%20Guide.pdf).
5
6
7 Dozier, J. (1989). "Spectral Signature of Alpine Snow Cover from the Landsat Thematic
8 Mapper." *Remote Sensing of Environment* **28**: 9 -22.
9
10
11 Farinotti, D., Huss, M., Bauder, A. and Funk, M. (2009). "An estimate of the glacier ice
12 volume in the Swiss Alps." *Global and Planetary Change* **68**: 225 - 231.
13
14
15 Foster, L. A., Brock, B. W., Cutler, M. E. J. and Diotri, F. (2012). "A physically based
16 method for estimating supraglacial debris thickness from thermal band remote-sensing data."
17 *Journal of Glaciology* **58**(210): 677 - 690.
18
19
20 Frey, H., Paul, F. and Strozzi, T. (2012). "Compilation of a glacier inventory for the western
21 Himalayas from satellite data: methods, challenges, and results." *Remote Sensing of*
22 *Environment* **124**(0): 832-843. <http://dx.doi.org/10.1016/j.rse.2012.06.020>.
23
24
25 Fujii, Y. and Higuchi, K. (1977). "Statistical analyses of the forms of the glaciers in Khumbu
26 Himal." *Seppyo* **39**: 7 - 14.
27
28
29 Fujita, K. and Sakai, A. (2014). "Modelling runoff from a Himalayan debris-covered glacier."
30 *Hydrol Earth Syst Sci Discuss* **11**: 2441 - 2482.
31
32
33 Fujita, K., Suzuki, R., Nuimura, T. and Sakai, A. (2008). "Performance of ASTER and
34 SRTM DEMs, and their potential for assessing glacial lakes in the Lunana region, Bhutan
35 Himalaya." *J Glaciol* **54**(185): 220 - 228.
36
37
38 Gardelle, J., Arnaud, Y. and Berthier, E. (2011). "Contrasted evolution of glacial lakes along
39 the Hindu Kush Himalaya mountain range between 1990 and 2009." *Global and Planetary*
40 *Change* **75**(1-2): 47 - 55. [10.1016/j.gloplacha.2010.10.003](https://doi.org/10.1016/j.gloplacha.2010.10.003).
41
42
43 Gardelle, J., Berthier, E. and Arnaud, Y. (2012a). "Slight mass gain of Karakoram glaciers in
44 the early twenty-first century, *Nature Geoscience*." *Nature Geoscience* **5**: 322 - 325.
45
46
47 Gardelle, J., Berthier, E., Arnaud, Y. and Kaab, A. (2013). "Region-wide glacier mass
48 balances over the Pamir-Karakoram-Himalaya during 1999-2011." *The Cryosphere* **7**(4):
49 1263 - 1286, doi:1210.5194/tc-1267-1263-2013.
50

1
2 Gardelle, J. E., Berthier, E. and Y.Arnaud (2012b). "Impact of resolution and radar
3 penetration on glacier elevation changed computed from DEM differencing." Journal of
4 Glaciology **58**(208): 419 - 422.
5
6
7 Hall, D. K., G. Riggs, A. and Salomonson, V. V. (1995). "Development of methods for
8 mapping global snow cover using moderate resolution imaging spectroradiometer data." Rem
9 Sens Environ **54**: 127 - 140.
10
11
12 Huss, M. and Farinotti, D. (2012). "Distributed ice thickness and volume of all glaciers
13 around the globe." Journal of Geophysical Research **117**(F04010). DOI:
14 10.1029/2012JF002523.
15
16
17 Imd. (1980). Climatological tables 1951 - 1980. Government of India, Controller of
18 Publication, New Delhi, pp.
19
20
21 Immerzeel, W., Van Beek, L. P. H. and Bierkens, M. F. P. (2010). "Climate Change Will
22 Affect the Asian Water Towers." Science **328**(5984): 1382-1385. 10.1126/science.1183188.
23
24
25 Immerzeel, W. W., Beek, L. P. H. V., Konz, M., Shrestha, A. B. and Bierkens, M. F. P.
26 (2012). "Hydrological response to climate change in a glacierized catchment in the
27 Himalayas." Climatic Change **110**(DOI 10.1007/s10584-011-0143-4): 721 - 736.
28
29
30 Iwata, S., Aoki, T., Kadota, T., Seko, K. and Yamaguchi, S. (2000). Morphological evolution
31 of the debris cover on Khumbu Glacier, Nepal, between 1978 and 1995. in: Debris-covered
32 glaciers. M. Nakawo, C.F. Raymond and A. Fountain (Eds.), IAHS. **264**: 3 - 11,
33
34
35 Kääb, A., Berthier, E., Nuth, C., Gardelle, J. and Arnaud, Y. (2012). "Contrasting patterns of
36 early twenty-first-century glacier mass change in the Himalayas." Nature **488**(7412): 495-
37 498.
38 [http://www.nature.com/nature/journal/v488/n7412/abs/nature11324.html#supplementary-](http://www.nature.com/nature/journal/v488/n7412/abs/nature11324.html#supplementary-information)
39 [information.](http://www.nature.com/nature/journal/v488/n7412/abs/nature11324.html#supplementary-information)
40
41
42 Kääb, A., Paul, F., Maisch, M., Hoelzle, M. and Haeberli, W. (2002). "The new remote-
43 sensing-derived Swiss glacier inventory: II. First results." Annals of Glaciology **34**: 362 -
44 366.
45
46
47 Kamp, U., Byrne, M. and Bolch, T. (2011). "Glacier fluctuations between 1975 and 2008 in
48 the Greater Himalaya Range of Zaskar, southern Ladakh." Journal of Mountain Sciences
49 **8**(3): 374 - 389.
50

1
2 Karma, Ageta, Y., Naito, N., Iwata, S. and Yabuki, H. (2003). "Glacier distribution in the
3 Himalayas and glacier shrinkage from 1963 to 1993 in the Bhutan Himalayas." *Bulletin of*
4 *Glaciological Research* **20**: 29 - 40.
5
6
7 Kaser, G., Grosshauser, M. and Marzeion, B. (2010). "Contribution potential of glaciers to
8 water availability in different climate regimes." *Proceedings of the National Academy of*
9 *Sciences of the United States of America* **107**(47): 20223-20227. Doi
10 10.1073/Pnas.1008162107.
11
12
13 Kayastha, R. B., Takeuchi, Y., Nakawo, M. and Ageta, Y. (2000). Practical prediction of ice
14 melting beneath various thickness of debris cover on Khumbu Glacier, Nepal, using a
15 positive degree-day factor. in: *Debris-Covered Glaciers*. C.F. Raymond, Nakawo, M.,
16 Fountain, A. (Eds.). Wallingford, UK, IAHS. **264**: 71 - 81,
17
18
19 Krishna, A. P. (2005). "Snow and glacier cover assessment in the high mountains of Sikkim
20 Himalaya." *Hydrological Processes* **19**(12): 2375-2383.
21
22
23 Kulkarni, A. V. (1992b). "Glacier inventory in the Himalaya." *Natural resources management*
24 *-a new perspective, NNRMS Bangalore*: pp. 474-478.
25
26
27 Kulkarni, A. V., Bahuguna, I. M., Rathore, B. P., Singh, S. K., Randhawa, S. S., Sood, R. K.
28 and Dhar, S. (2007). "Glacial retreat in Himalaya using Indian Remote Sensing satellite
29 data." *Current Science* **92**(1): 69-74.
30
31
32 Loibl, D. M., Lehmkuhl, F. and Griebinger, J. (2014). "Reconstructing glacier retreat since
33 the Little Ice Age in SE Tibet by glacier mapping and equilibrium line altitude calculation."
34 *Geomorphology* **214**: 22 - 39. doi:10.1016/j.geomorph.2014.03.018.
35
36
37 Manley, W. F. (2008). Geospatial inventory and analysis of glaciers: A case study for the
38 eastern Alaska Range, in *Glaciers of Alaska*. in: *Satellite Image Atlas of Glaciers of the*
39 *World: USGS Professional Paper 1386-K*. R. S. Williams, Jr., and Ferrigno, J. G. (Eds.),
40
41
42 Mason, L. E. (1954). *Abode of Snow: A History of Himalayan Exploration and*
43 *Mountaineering*. Dutton, New York City.
44
45
46 Mihalcea, C., Mayer, C., Diolaiuti, G., D'agata, C., Smiraglia, C., Lambrecht, A., Vuillermoz,
47 E. and Tartari, G. (2008a). "Spatial distribution of debris thickness and melting from remote-
48 sensing and meteorological data, at debris-covered Baltoro glacier, Karakoram, Pakistan."
49 *Annals of Glaciology* **48**(1): 49-57.
50

1
2 Mihalcea, C. E., Brock, B. W., Diolaiuti, G. A., D'agata, C., Citterio, M., Kirkbride, M. P.,
3 Cutler, M. and Smiraglia, C. (2008b). "Using ASTER satellite and ground-based surface
4 temperature measurements to derive supraglacial debris cover and thickness patterns on
5 Miage Glacier (Mont Blanc Massif, Italy)." *Cold Regions Science and Technology* **52**(3):
6 341 - 354. doi:10.1016/j.coldregions.2007.03.004.
7
8
9 Mool, P. K. and Bajracharya, S. R. (2003). Tista Basin, Sikkim Himalaya: Inventory of
10 Glaciers and Glacial Lakes and the Identification of Potential Glacial Lake Outburst Floods
11 (GLOFs) Affected by Global Warming in the Mountains of Himalayan Region. International
12 Center for Integrated Mountain Development, Kathmandu, Nepal, 145 pp.
13
14
15 Mool, P. K., Bajracharya, S. R., Joshi, S. P., Sakya, K. and Baidya, A. (2002). Inventory of
16 Glaciers, Glacial Lakes and Glacial Lake Outburst Floods Monitoring and Early Warning
17 Systems in the Hindu-Kush Himalayan region, Nepal, International Center for Integrated
18 Mountain Development, Nepal.
19
20
21 Nandy, S. N., Dhyani, P. P. and Samal, P. K. (2006) "Resource Information database for the
22 Indian Himalaya, ENVIS Monograph No. 3
23 <http://gbpihedenvi.nic.in/HTML/monograph3/Contents.html>." Last accessed: 2014-07-01.
24
25
26 Narama, C., Käab, A., Kajiura, T. and Abdrakhmatov, K. (2007). "Spatial variability of
27 recent glacier area and volume changes in Central Asia using Corona, Landsat, ASTER and
28 ALOS optical satellite data." *Geophys Res Abstr* **9**(08178).
29
30
31 Nuimura, T., Fujita, K., Yamaguchi, S. and Sharma, R. R. (2012). "Elevation changes of
32 glaciers revealed by multitemporal digital elevation models calibrated by GPS survey in the
33 Khumbu region, Nepal Himalaya, 1992-2008." *Journal of Glaciology* **58**(210): 648-656.
34
35
36 Nuimura, T., Sakai, A., Taniguchi, K., Nagai, H., Lamsal, D., Tsutaki, S., Kozawa, A.,
37 Hoshina, Y., Takenaka, S., Omiya, S., Tsunematsu, K., Tshering, P. and Fujita, K. (2014).
38 "The GAMDAM Glacier Inventory: a quality controlled inventory of Asian glaciers." *The*
39 *Cryosphere Discuss*, www.the-cryosphere-discuss.net/1/77/2007/ **8**(doi:10.5194/tcd-8-2799-
40 2014): 2799 - 2829.
41
42
43 Nuth, C. and Käab, A. (2011). "Co-registration and bias corrections of satellite elevation data
44 sets for quantifying glacier thickness change." *The Cryosphere*(5): 271 - 290.
45
46
47 Palazzi, E., Von Hardenberg, J. and Provenzale, A. (2013). "Precipitation in the Hindu-Kush
48 Karakoram Himalaya: Observations and future scenarios." *Journal of Geophysical Research:*
49 *Atmospheres* **118**(1): 85-100. 10.1029/2012jd018697.
50

1
2 Paterson, W. S. B. (1994). *The Physics of Glaciers*, 3rd ed. Oxford, Pergamon.
3
4
5 Paul, F., Barrand, N., Berthier, E., Bolch, T., Casey, K., Frey, H., Joshi, S. P., Kononov, V.,
6 Bris, R. L., Mölg, N., Nosenko, G., Nuth, C., Pope, A., Racoviteanu, A., Rastner, P., Raup,
7 B., Scharrer, K., Steffen, S. and Winsvold, S. (2013). "On the accuracy of glacier outlines
8 derived from remote sensing data." *Annals of Glaciology* **54**(63). 10.3189/2013AoG63A296.
9
10
11 Pfeffer, W. T., Arendt, A. A., Bliss, A., Bolch, T., Cogley, J. G., Gardner, A. S., Hagen, J. O.,
12 Hock, R., Kaser, G., Kienholz, C., Miles, E. S., Moholdt, G., Mölg, N., Paul, F., Radić, V.,
13 Rastner, P., Raup, B. H., Rich, J., Sharp, M. J. and Randolph_Consortium (2014). "The
14 Randolph Glacier Inventory: a globally complete inventory of glaciers." *Journal of*
15 *Glaciology* **60**(221). doi: 10.3189/2014JoG13J176.
16
17
18 Racoviteanu, A., Armstrong, R. and Williams, M. (2013a). "Evaluation of an ice ablation
19 model to estimate the contribution of melting glacier ice to annual discharge in the Nepal
20 Himalaya." *Water Resources Research* **49**(9): 5117 - 5133. DOI: 10.1002/wrcr.20370.
21
22
23 Racoviteanu, A., Arnaud, Y., Baghuna, I. M., Bajracharya, S., Berthier, E., Bhambri, R.,
24 Bolch, T., Byrne, M., Chaujar, R. K., Käab, A., Kamp, U., Kargel, J., Kulkarni, A. V.,
25 Leonard, G., Mool, P., Frauenfelder, R. and Sossna, I. (2014). Himalayan glaciers. in: *Global*
26 *Land and Ice Monitoring from Space: Satellite Multispectral Imaging of Glaciers*. Jeffrey S.
27 Kargel, Michael P. Bishop, Andreas Käab and Bruce H. Raup (Eds.). Heidelberg, Springer-
28 Praxis: 549 - 582, 978-3-540-79817-0, "10.1007/978-3-540-79818-7:" 10.1007/978-3-540-
29 79818-7.
30
31
32 Racoviteanu, A., Arnaud, Y. and Williams, M. (2008a). "Decadal changes in glacier
33 parameters in Cordillera Blanca, Peru derived from remote sensing." *J Glaciol* **54**(186): 499 -
34 510.
35
36
37 Racoviteanu, A., Nicholson, L. and Arnaud, Y. (2013b). Surface characteristics of debris-
38 covered glacier tongues in the Khumbu Himalaya derived from remote sensing texture
39 analysis. European Geophysical Union (EGU) General Assembly. Vienna, Austria. **15**:
40 10174.
41
42
43 Racoviteanu, A., Paul, F., Raup, B., Khalsa, S. J. S. and Armstrong, R. (2009). "Challenges
44 and recommendations in mapping of glacier parameters from space: results of the 2008 Global
45 Land Ice Measurements from Space (GLIMS) workshop, Boulder, Colorado, USA." *Annals*
46 *of Glaciology* **50**(53): 53 - 69.
47
48

- 1 Racoviteanu, A., Williams, M. W. and Barry, R. (2008b). "Optical remote sensing of glacier
2 mass balance: a review with focus on the Himalaya." *Sensors* **Special issue: Remote sensing
3 of the environment**(8): 3355 - 3383.
4
5
- 6 Racoviteanu, A. E. and Williams, M. W. (2012). "Decision tree and texture analysis for
7 mapping debris-covered glaciers: a case study from Kanchenjunga, eastern Himalaya."
8 *Remote Sensing Special issue* **4**(10): 3078-3109, doi:3010.3390/rs4103078.
9
10
- 11 Raj, K. B. G., Remya, S. N. and Kumar, K. V. (2013). "Remote sensing-based hazard
12 assessment of glacial lakes in Sikkim Himalaya." *Current Science* **104**(3): 359 - 364.
13
14
- 15 Raup, B. H., Käab, A., Kargel, J. S., Bishop, M. P., Hamilton, G., Lee, E., Paul, F., Rau, F.,
16 Soltész, D., Khalsa, S. J. S., Beedle, M. and Helm, C. (2007). "Remote sensing and GIS
17 technology in the Global Land Ice Measurements from Space (GLIMS) Project." *Computers
18 and Geosciences* **33**: 104-125.
19
20
- 21 Raup, B. H. and Khalsa, S. J. S. (2007). "GLIMS Analysis tutorial." GLIMS. Last accessed:
22 04-01-2014, from
23 http://www.glims.org/MapsAndDocs/assets/GLIMS_Analysis_Tutorial_a4.pdf.
24
25
- 26 Rees, W. G. (2003). *Remote sensing of snow and ice*, Taylor & Francis Group, Boca Raton
27 FL.
28
29
- 30 Sakai, A. and Fujita, K. (2010). "Correspondence: Formation conditions of supraglacial lakes
31 on debris covered glaciers in the Himalaya." *Journal of Glaciology* **56**(195): 177 - 181.
32
33
- 34 Sakai, A., Nakawo, M. and Fujita, K. (2002). "Distribution Characteristics and Energy
35 Balance of Ice Cliffs on Debris-Covered Glaciers, Nepal Himalaya." *Arctic Antarctic and
36 Alpine Research* **34**(1): 12 - 19.
37
38
- 39 Salerno, F., Buraschi, E., Bruccoleri, G., G. Tartari and C. Smiraglia (2008). "Glacier surface-
40 area changes in Sagarmatha national park, Nepal, in the second half of the 20th century, by
41 comparison of historical maps." *Journal of glaciology* **54**(187): 738 - 752.
42
43
- 44 Salerno, F., Thakuri, S., D'agata, C., Smiraglia, C., Manfredi, E. C., Viviano, G. and Tartari,
45 G. (2012). "Glacial lake distribution in the Mount Everest region: Uncertainty of
46 measurement and conditions of formation." *Global and Planetary Change* **92-93**: 30-39.
47
48

- 1 Sangewar, C. V. and Shukla, S. P., Eds. (2009). Inventory of Himalayan glaciers: A
2 Contribution to the International Hydrological Programme. Calcutta, Geological Survey of
3 India (GSI Special Publication 34): An updated edition. 594 pp.
4
5
6 Scherler, D., Bookhagen, B. and Strecker, M. R. (2011). "Spatially variable response of
7 Himalayan glaciers to climate change affected by debris cover." *Nature Geosci* **4**(3): 156-
8 159. [http://www.nature.com/ngeo/journal/v4/n3/abs/ngeo1068.html#supplementary-](http://www.nature.com/ngeo/journal/v4/n3/abs/ngeo1068.html#supplementary-information)
9 [information](http://www.nature.com/ngeo/journal/v4/n3/abs/ngeo1068.html#supplementary-information).
10
11
12 Shanker, R. (2001). Glaciological studies in India, a contribution from Glaciological Survey
13 of India. . Symposium on snow, ice and glacier, March 1999, Geological Survey of India
14 Special Publication. 53, 11 - 15.
15
16
17 Shrestha, A., C.P.Wake, Dibb, J. E. and Mayevski, P. A. (2000). "Precipitation fluctuations in
18 the Nepal Himalaya and its vicinity and relationship with some large-scale climatologic
19 patterns." *Int J Climatol* **20**: 317 - 327.
20
21
22 Srikantia, S. V. (2000). "Restriction on maps: A denial of valid geographic information."
23 *Current Science* **79**(4): 484 - 488.
24
25
26 Survey_of_India (2005). "National Map Policy." Survey of India. Last accessed: 2014 - 06
27 - 01, 2014, from
28 <http://www.surveyofindia.gov.in/tenders/nationalmappolicy/nationalmappolicy.pdf>.
29
30
31 Thakuri, S., Salerno, F., C.Smiraglia, T.Bolch, D'agata, C., G.Viviano and Tartari, G. (2014).
32 "Tracing glacier changes since the 1960s on the south slope of Mt. Everest (central Southern
33 Himalaya) using optical satellite imagery." *The Cryosphere* **8**: 1297 - 1315. doi:10.5194/tc-8-
34 1297-2014.
35
36
37 Usgs-Eros (1996). "USGS Declassified Imagery-1 ". Last accessed: 03-01, 2012, from
38 <http://eros.usgs.gov/#/Guides/displ>.
39
40
41 Wagnon, P., Vincent, C., Arnaud, Y., Berthier, E., Vuillermoz, E., Gruber, S., Ménégoz, M.,
42 Gilbert, A., Dumont, M. and Pokharel, B. (2013). "Seasonal and annual mass balances of
43 Mera and Pokalde glaciers (Nepal Himalaya) since 2007." *The Cryosphere*.
44
45
46 Wessels, R. L., Kargel, J. S. and Kieffer, H. H. (2002). ASTER measurement of supraglacial
47 lakes in the Mount Everest region of the Himalaya. in: *Annals of Glaciology*, Vol 34,
48 2002(Eds.). **34**: 399-408,
49
50

1 Yanai, M., Li, C. and Z.Song (1992). "Seasonal heating of the Tibetan plateau and its effect
 2 on the evolution of the Asian summer monsoon." J. Meteorol. Soc. Jpn **70**: 319 - 351.

3
 4
 5 Zhang, Y., Fujita, K., Liu, S., Liu, Q. and Nuimura, T. (2011). "Distribution of debris
 6 thickness and its effect on ice melt at Hailuogou glacier, southeastern Tibetan Plateau, using
 7 in situ surveys and ASTER imagery." Journal of Glaciology **57**(206): 1147-1157.

8
 9
 10 **Tables**

11
 12 **Table 1.** Summary of satellite imagery used in this study
 13
 14
 15

Sensor	Scene ID	Date	Spatial resolution	Image type
Corona KH4	DS009048070DA244	1962-10-25	7.5 m	Panchromatic
	DS009048070DA243			
	DS009048070DA242			
Landsat ETM+	L7CPF20001001_20001231_07	2000-12-26	15 m	Panromatic
			28.5 m	Visible,shortwave
			90 m	Thermal infrared
ASTER	AST_L1A#003_12012000051205_072 92001131755	2000-12-01	15 m 30 m 90 m	Visible Shortwave Thermal infrared
	AST_L1A#003_12012000051214_072 92001131813	2000-12-01		
	AST_L1A_00311272001045729_0222 2004173619	2001-11-27		
	AST_L1A#00301052002050207_0130 2002193030	2002-01-05		
	AST_L1A#00301052002050216_0130 2002193046	2002-01-05		
	AST_08_00310292002045428_201012 12181710_16443	2002-10-29		
QuickBird	1010010004BD8700	2006-01-01	2.4 m	Visible, shortwave
	1010010004BB8F00	2006-01-06		
WorldView -2	102001000FBA1D00	2010-12-02	.50 m	Panchromatic
	102001000586E700	2009-12-01		

1
2
3

Table 2. Spatial domains used for analysis and their characteristics

Spatial domain	Number of glaciers	Area in 2000 (km²)	Details
1. Landsat/ ASTER extent	487	1463 ± 88	The area of the Eastern Himalaya extending from Sikkim to China, as well as parts of W Bhutan and E Nepal
2. Corona extent	232	777 ± 46	Glaciers of Eastern Nepal (Tamor basin) and Sikkim
3. Quickbird extent	50	551 ± 34	Kanchenjunga-Sikkim area

4
5
6
7

Table 3. Topographic zones in spatial domain 1

	N side (China)	W side (Nepal)	E side (Sikkim)	E side (Bhutan)
Mean basin elevation (m)	4931	4819	4658	4491
Mean rainfall TRMM (mm/yr)	146	805	977	383

Table 4. Topographic parameters for glaciers in spatial domain 1 and sub-regions based on 2000s Landsat/ASTER analysis. All parameters are presented on a) region-by-region and b) glacier-by-glacier basis from the SRTM DEM. Debris cover fraction is calculated as % glacier area of debris covered glaciers only.

Parameter	All	Nepal	Sikkim	Bhutan	China
<i>a) Region-wide averages</i>					
Number of glaciers	487	162	186	30	109
Glacierized area (km ²)	1463 ± 88	488 ± 29	569±34	106 ± 6	300±18
Number of debris-covered tongues	68	30	27	7	4
Debris cover area (km ²)	161±10	64±4	78±5	14±1	6±0.4
Debris cover (% total glacier area)	11	13	14	13	2
<i>b) Glacier averages</i>					
Minimum elevation (m)	4908	4760	4702	4926	5425
Median elevation (m)	5702	5715	5569	5652	5950
Maximum elevation (m)	6793	6928	6908	6685	6530
Slope (degree)	23	24	23	27	21
Aspect (degree)	177	236	131	134	180
Mean glacier size (km ²)	3	3	3	4	3
Length (km)	2	2	2	3	2
Thickness (m)	24	23	23	31	27
Debris cover fraction (%)	23	21	23	32	17

Table 5. Overall glacier area changes east to west for the 232 glaciers in spatial domain 2 from 1962 (Corona) to 2000 (Landsat/ASTER).

Sub-region	Area (km ²)		Area loss 1962 - 2000		
	1962	2000	km ²	%	% yr ⁻¹
Nepal	323.9±10	269.1±16	54.8±19	16.9±6	0.44±0.2
Sikkim	634.7±19	507.0±35	127.7±42	20.1±8	0.52±0.2
All spatial domain	958.7±31	776.1±47	182.5±40	19.0±4	0.50±0.1

Table 6. Glacier area change for debris-covered versus clean glaciers in spatial domain 2 from 1962 to 2000. Change is shown as percent of glacier area on a glacier-by-glacier basis.

Glacier type/ Sub-region	Sikkim		Nepal		All	
	Number of glaciers	Area loss (%)	Number of glaciers	Area loss (%)	Number of glaciers	Area loss (%)
Clean glaciers	144	34.7	53	31.6	197	33.9
Debris-covered glaciers	20	20.8	15	23.8	35	22.1
Both types	164	33.0	68	29.9	232	32.1

Table 7 Linear regression of area change on topographic and climatic variables for the 232 glaciers in the spatial domain 2

Regression	Coefficient	P-value
Glacier area	-0.47	0.0003**
Altitudinal range	-0.01	<0.001**
Minimum elevation	0.008	0.02*
Median elevation	-0.01	0.001**
Maximum elevation	-0.01	<0.001**
Percent debris	-0.004	0.83
Slope	0.47	0.01*
Aspect	0.03	0.007**
Solar radiation	0.01	0.74
Precipitation	-0.002	0.26

* Significant at the 0.05 level (2-tailed).

** Significant at the 0.01 level (2-tailed).

Table 8. Comparison of glacier parameters for clean glaciers versus debris-covered glaciers

Parameter	Clean glaciers	Debris-covered glaciers
Area (km ²)	1.2	15.0
Area change (%)	33.9	22.1
Slope	25.8	24.5
Minimum elevation (m)	5105.6	4714.2
Median elevation (m)	5424.5	5538.9
Altitudinal range (m)	627.6	1928.6
Length (km)	1.3	6.7

Table 9 Glacier area change in Sikkim based on previous studies. The percent area change is given with respect to the 1962 Corona glacier inventory from this study.

Study	Year	Data source	Number of glaciers	Area (km ²)	Area change since 1960s	
					%	% yr ⁻¹
This study	1962	Corona KH4	178	658±20	-	-
Geological Survey of India (1999)	~1960-1970s	Indian 1:63,000 topographic maps	449	706	+7.3	+0.9
Kulkarni and Narain (1990)	1987/1989	IRS-1C satellite images	n/a	426	-35.0	-1.4
ICIMOD Mool et al, (2002)	2000	Landsat TM, IRS-1C, topographic maps	285	577	-11.4	-0.3
This study	2000	Landsat TM, ASTER	185	569±34	-13.5±6.4	-0.3±0.1

List of figures

Fig. 1 Location map of the study area. The images used in this study are shown as false color composites (Landsat 432, ASTER 321), overlaid on a hillshade of the SRTM DEM. Also shown are the spatial domain 1 (entire image extent), spatial domain 2 (solid yellow rectangle) and spatial domain 3 (dotted polygon).

Fig. 2 Precipitation regime over domain 1 expressed as rain rate, from the TRMM 2B31 data averaged for the period 1998 – 2010. The graph shows the monsoon period from June to September, with a peak precipitation in July, and the influence of the northeastern monsoon during the winter/early spring (January-March).

Fig. 3 Spatial patterns in TRMM annual precipitation rate derived from the 3B43 dataset for spatial domain 1. Also shown are the four main basins delineated based on topography and watershed functions. 2000 glacier outlines are shown in black. We note several cells of high precipitation at high altitudes over the Kanchenjunga summits and parts of Tibet, most likely errors in TRMM data.

Fig. 4 Frequency distribution of glacier parameters for the 487 glaciers in spatial domain 1 based on Landsat/ASTER analysis: a) area; b) slope; c) length and d) thickness. Glaciers smaller than 10 km² in area, < 2 km in length and <30 m thickness are prevalent, with an average slope of 23°.

Fig. 5 Aspect frequency distribution of the 487 glaciers in spatial domain 1 based on Landsat/ASTER analysis. On average, glaciers in this area are preferentially oriented towards NW (300°) and NE (60°).

Fig. 6 Spatial patterns in glacier median elevation derived from 2000 Landsat/ASTER outlines and SRTM DEM.

Fig. 7 Spatial patterns in glacier area change derived from 1962 Corona and 2000 Landsat/ASTER data, on a glacier-by-glacier basis.

Fig. 8 Dependency of glacier area change 1962 – 2000 on a) glacier altitudinal range (maximum – minimum elevation) and b) glacier area. Debris-covered glaciers are shown as grey solid circles; clean glaciers are shown as black solid triangles.

Fig. 9 Distribution of surface temperatures along longitudinal for selected debris-covered tongues in spatial domain 2. Temperatures are extracted from ASTER kinetic temperature data (AST08) from the Oct 29th, 2002 image.

Fig. 10 Surface temperature distribution along longitudinal transects from selected glaciers. Distance is measured from the upper part of the debris-covered area down glacier to the terminus. Labels point to: A- Kanchenjunga glacier, B- Yalung glacier and C- Zemu glacier.

Fig. 11 Area changes for some glaciers in the Zema Chhu basin Sikkim from 1962 to 2006: a) 1962 Corona-based glacier outlines (in blue) and b) 2006 QB glacier outlines (in orange).

Fig. 12 Close-up view of glacier area changes around the N. and S. Lhonak glaciers 1962 to 2006, showing changes in the pro-glacial lakes.

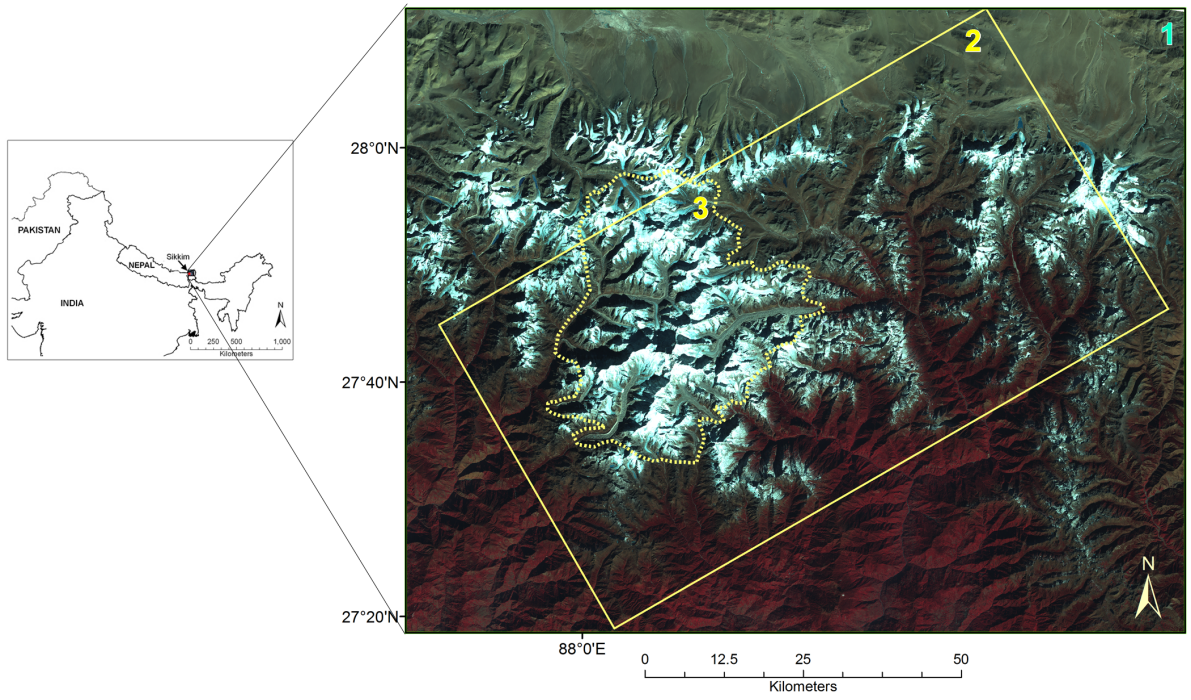


Fig.1

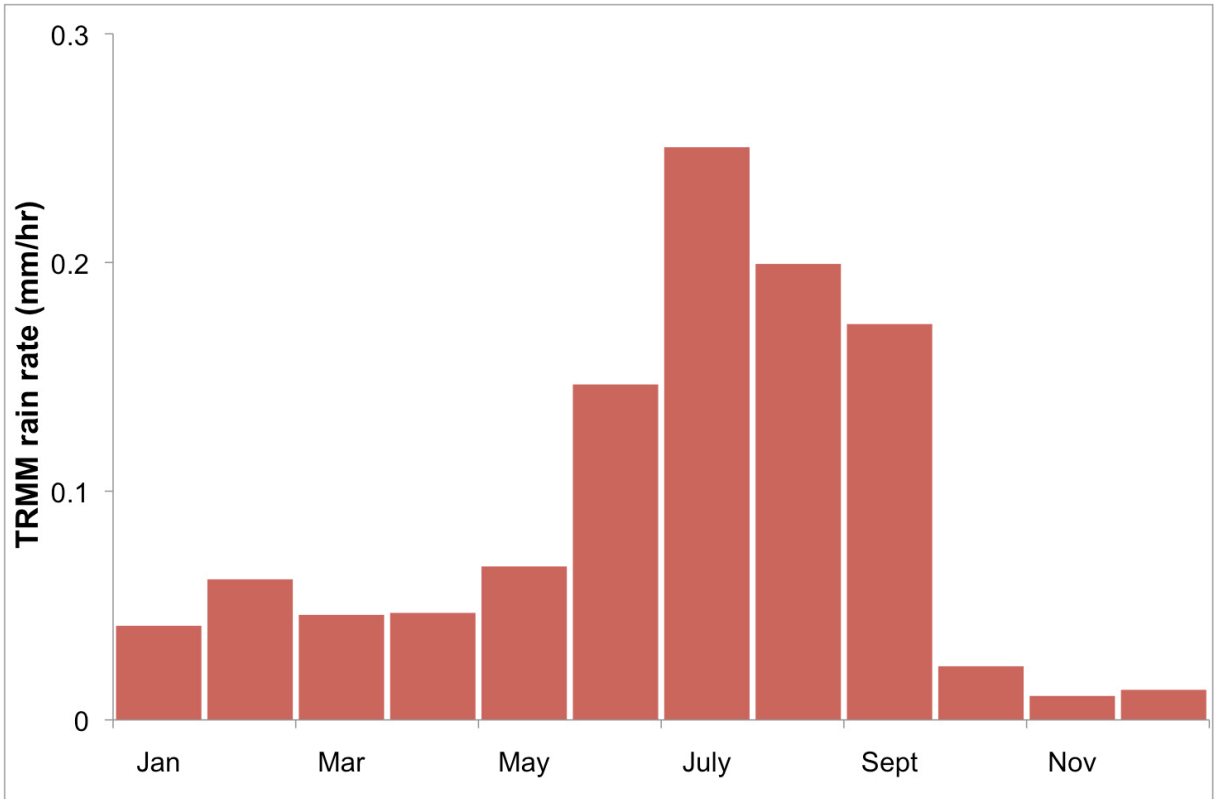


Fig. 2

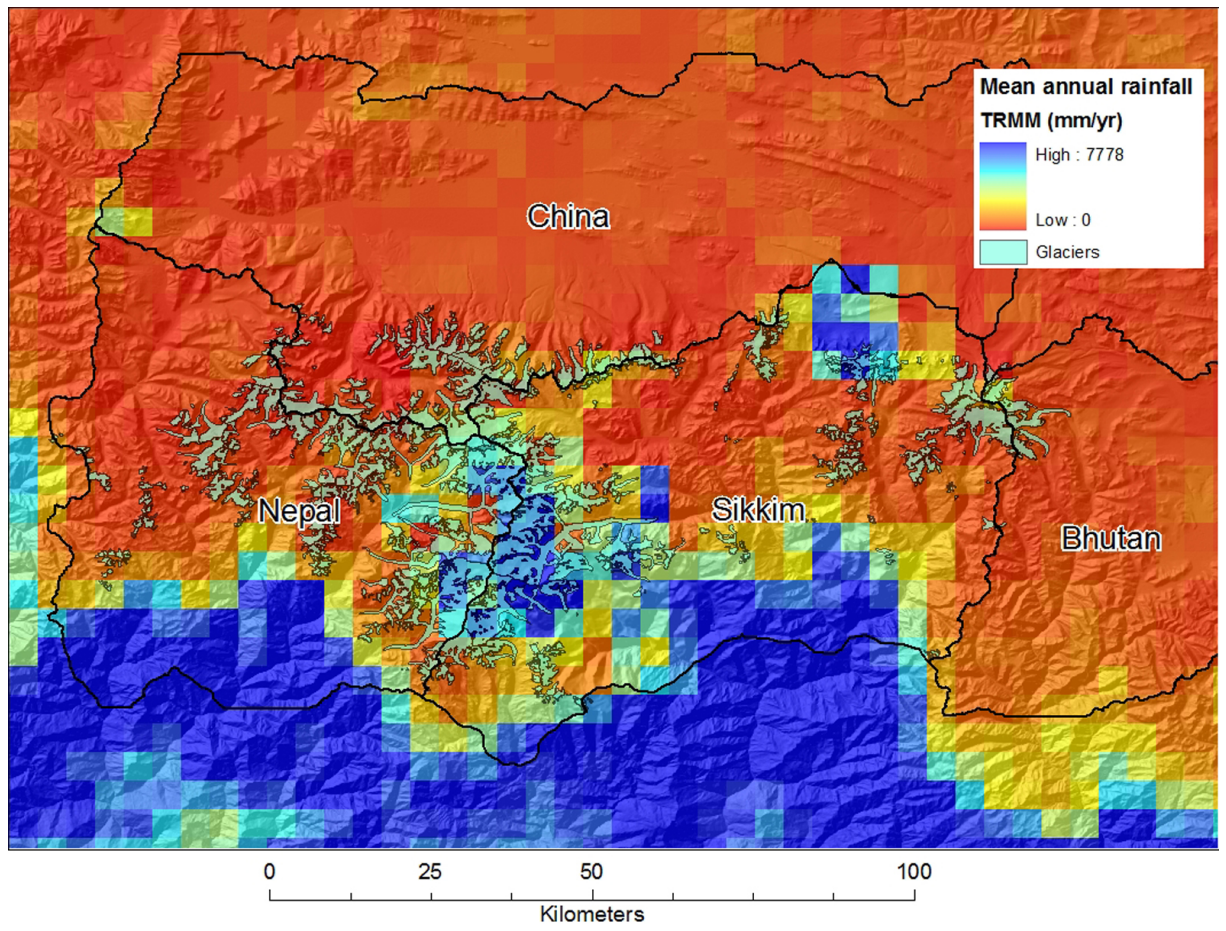


Fig.3

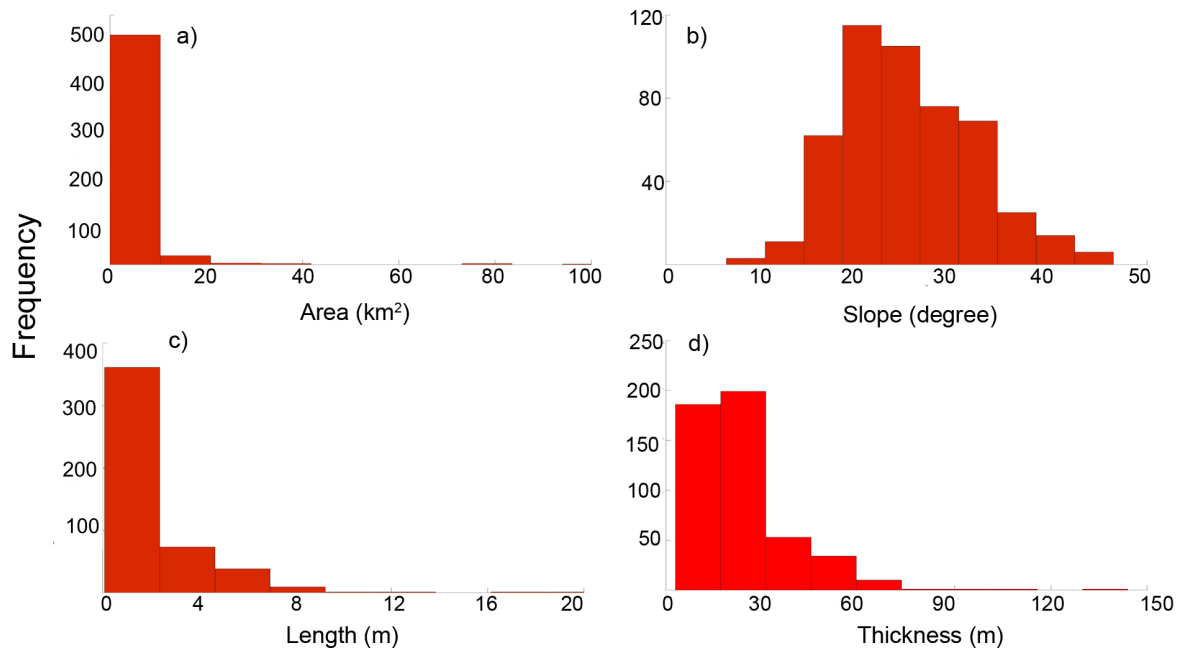


Fig. 4

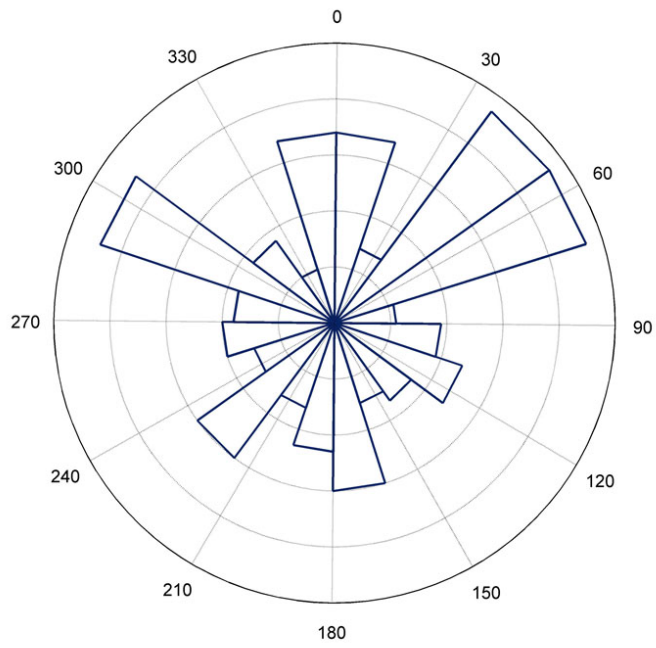


Fig. 5

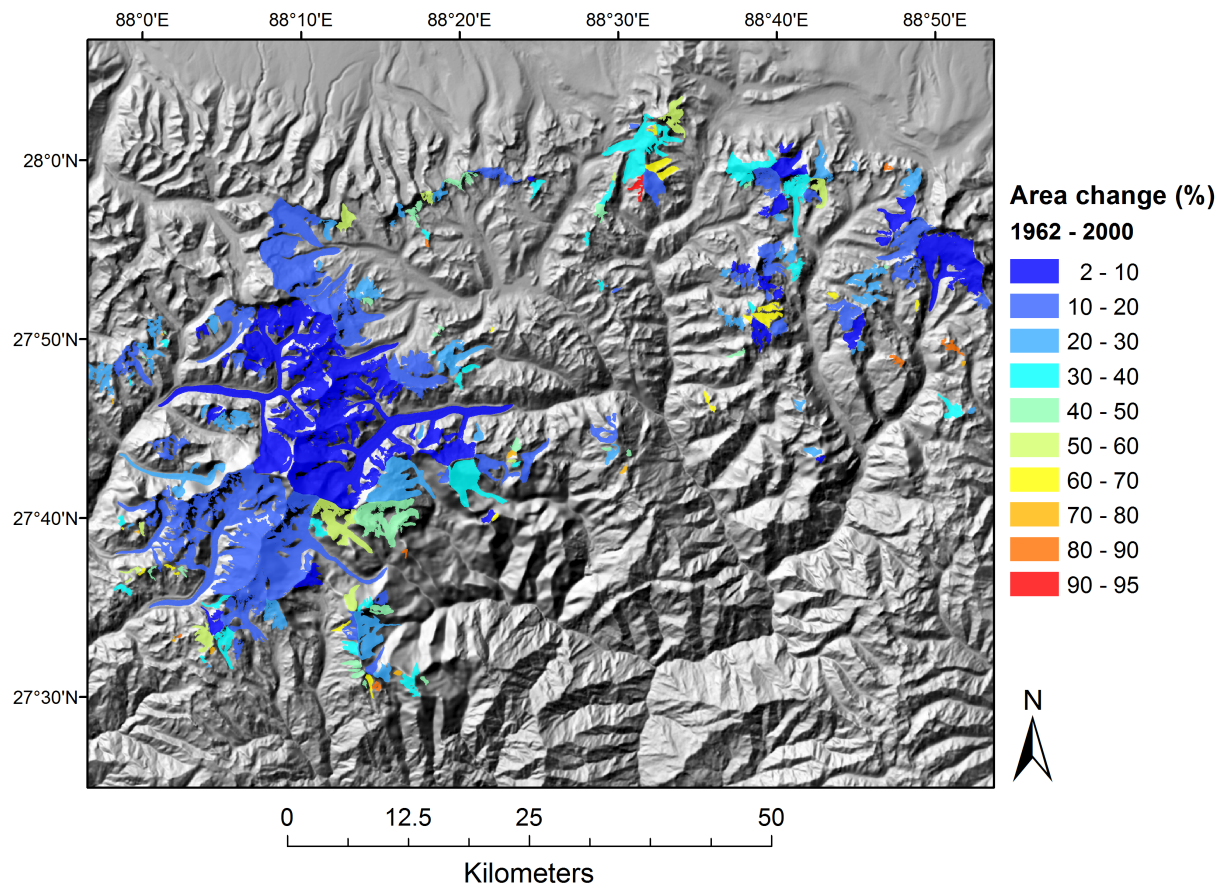


Fig. 6

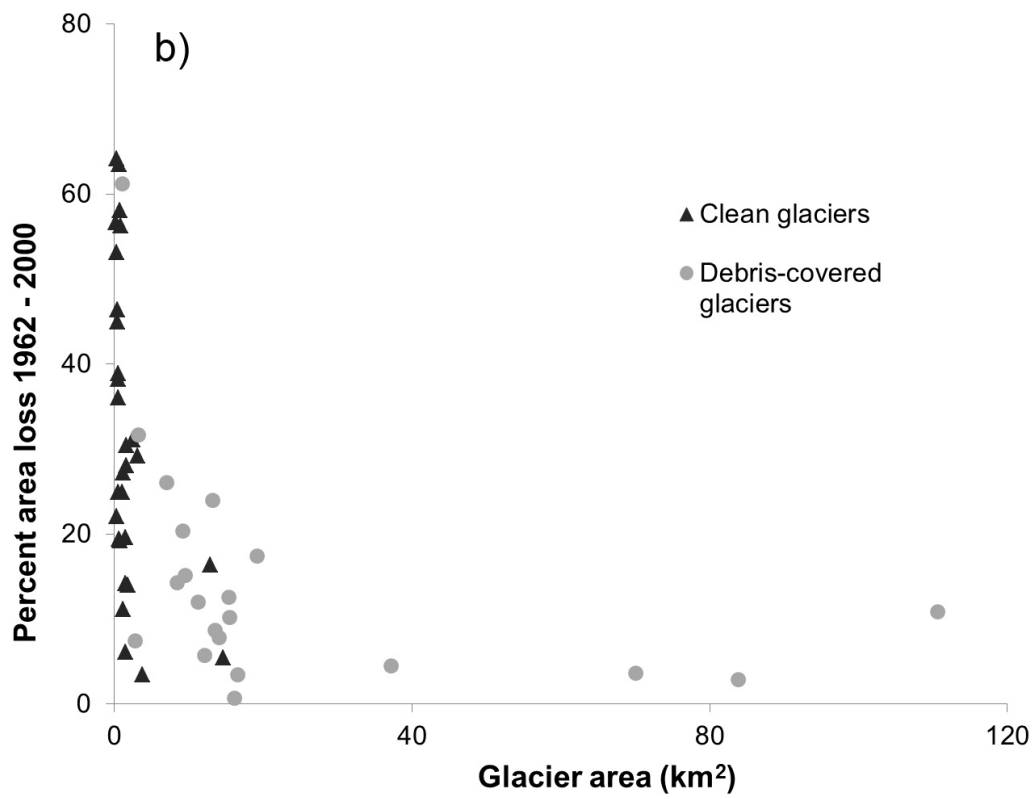
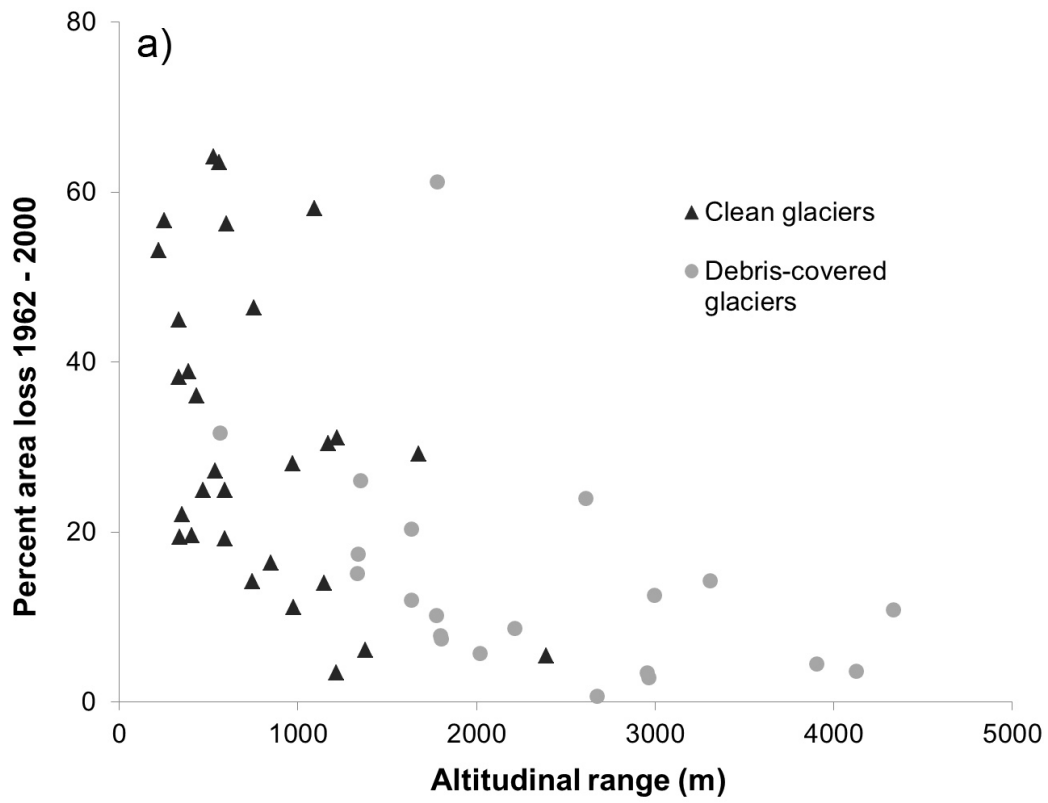


Fig. 7

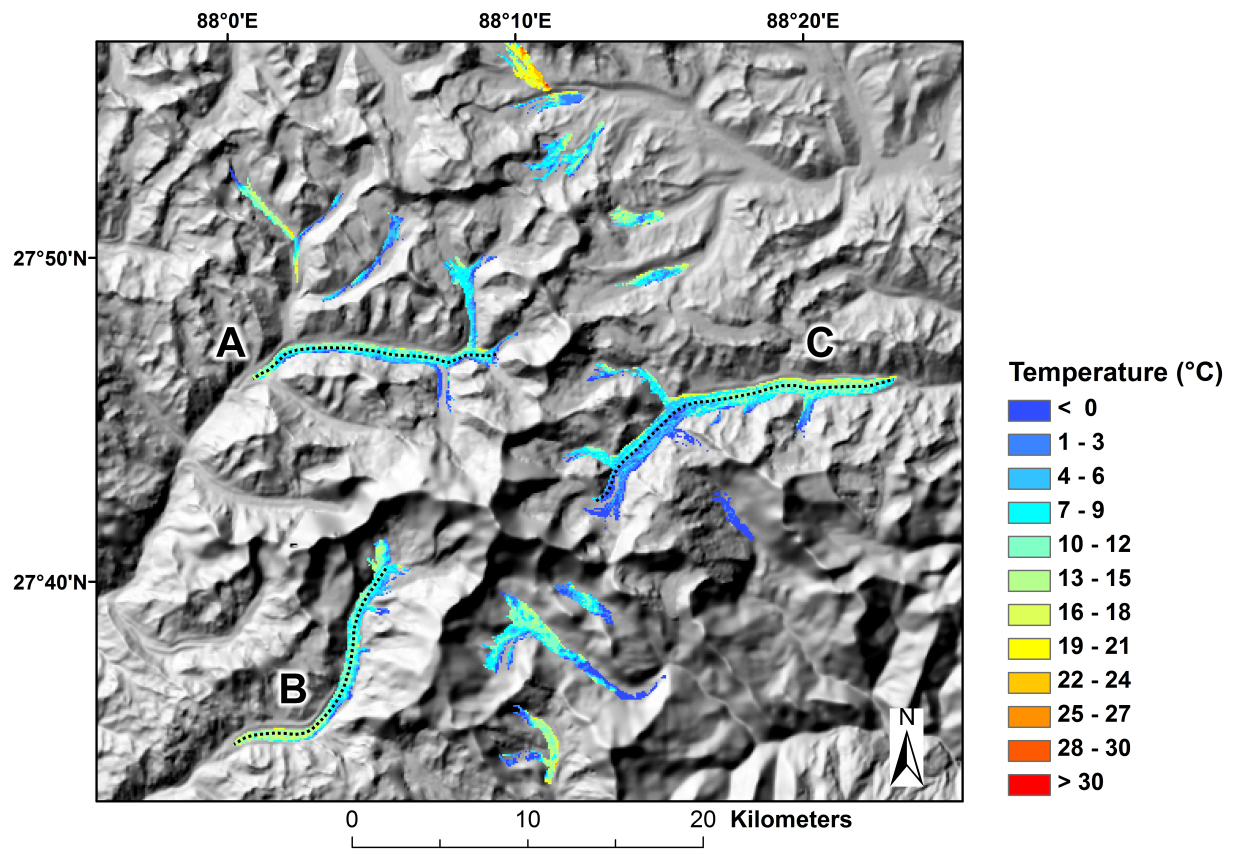


Fig. 8

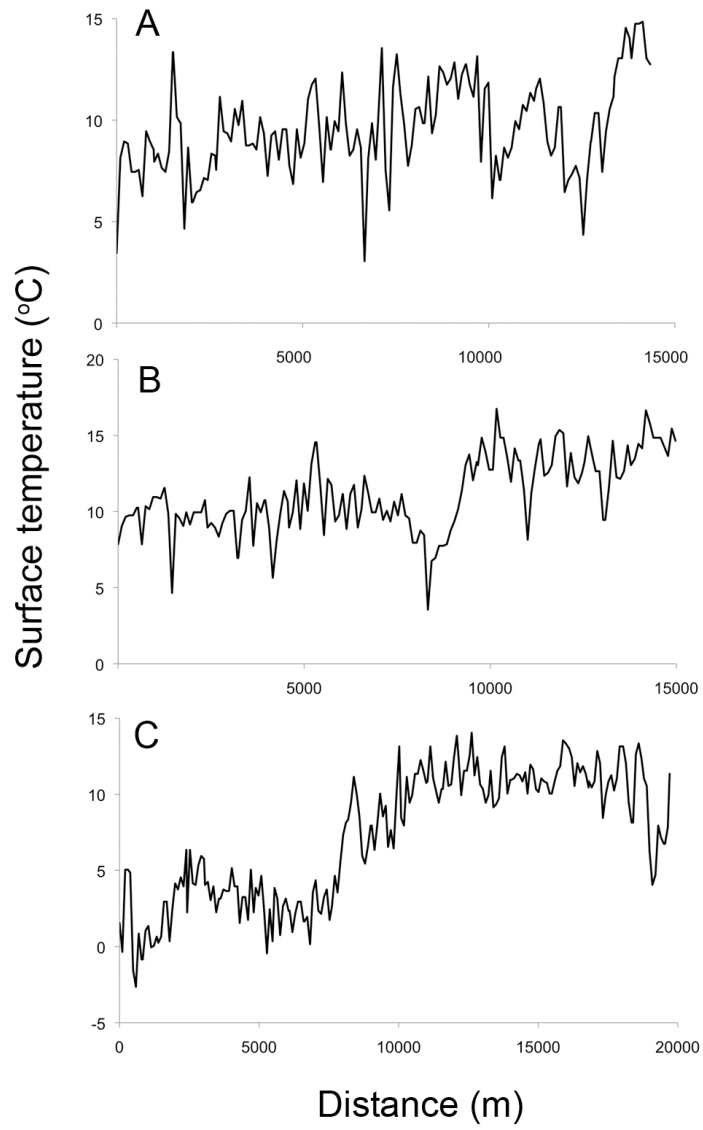


Fig. 9

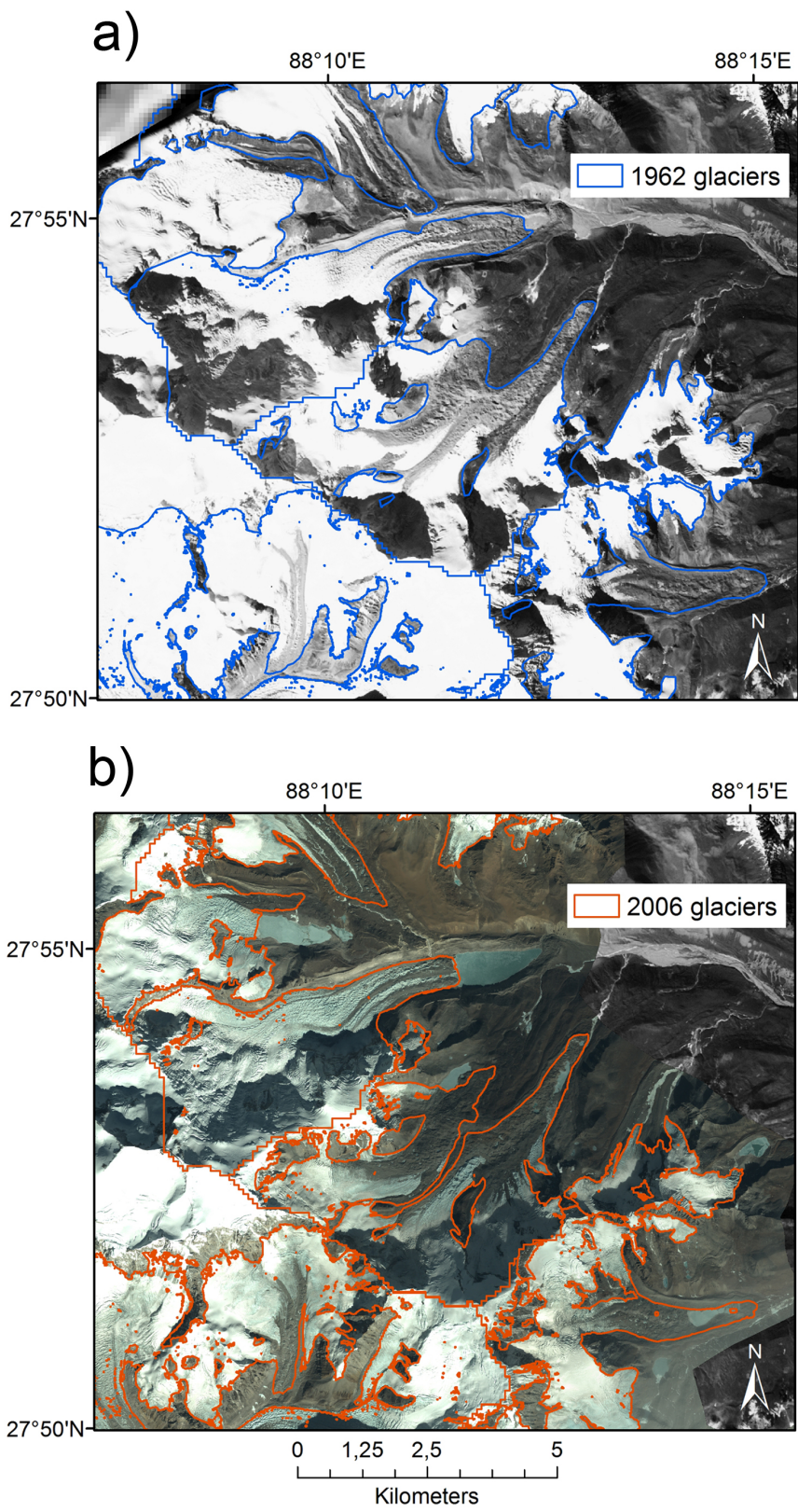


Fig. 10

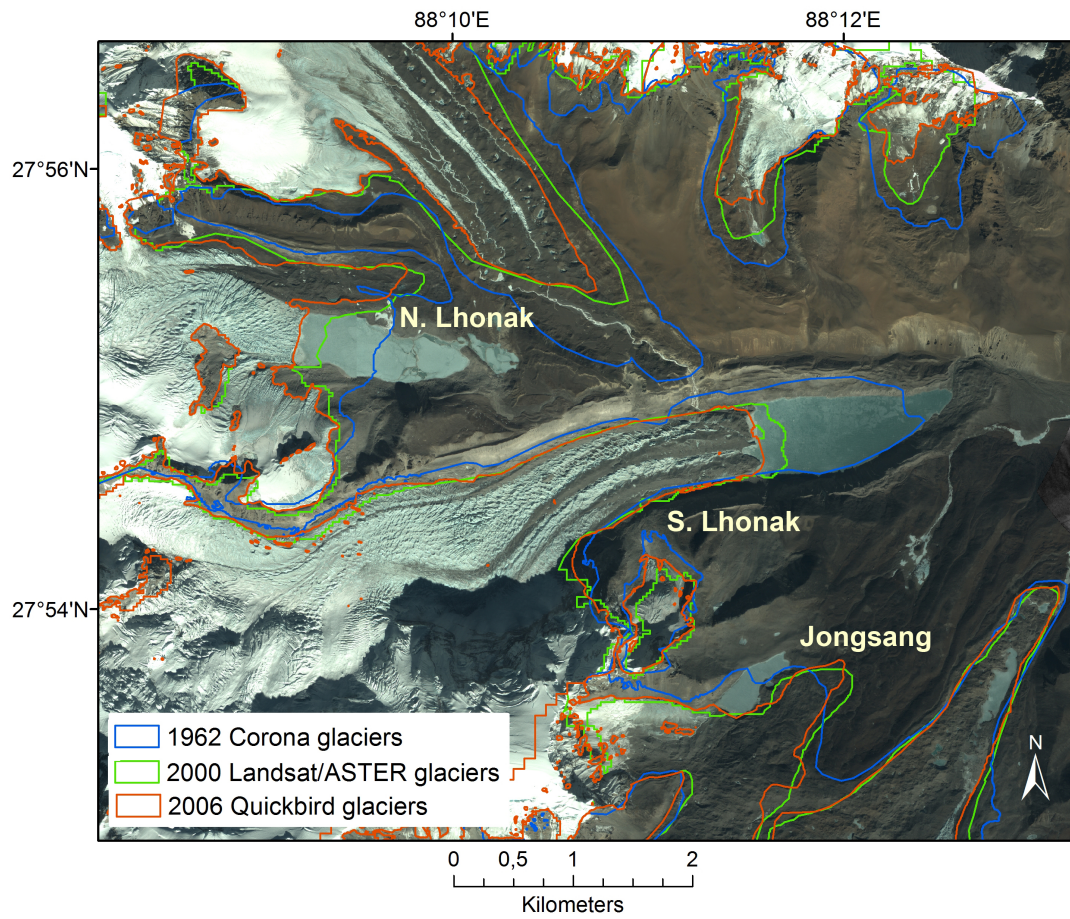


Fig. 11